Bioorganic Chemistry 97 (2020) 103708

Contents lists available at ScienceDirect

Bioorganic Chemistry

journal homepage: www.elsevier.com/locate/bioorg

Multiple molecular targets mediated antioxidant activity, molecular docking, ADMET, QSAR and bioactivity studies of halo substituted urea derivatives of α-Methyl-L-DOPA

Nagalakshmamma Vadabingi[a], Vijaya Kumar Reddy Avula[b], Grigory V. Zyryanov[b,c], Swetha Vallela[d], Jaya Shree Anireddy[d], Visweswara Rao Pasupuleti[e], Venkataswamy Mallepogu[f], Naga Raju Chamarthi[g,**], Venkata Chalapathi Ponne[a,*]

[a] Department of Chemistry, Tirumala Tirupati Devasthanam's Sri Venkateswara Arts College, Tirupati 517502, Andhra Pradesh, India
[b] Chemical Engineering Institute, Ural Federal University, Yekaterinburg 620002, Russian Federation
[c] Ural Division of the Russian Academy of Sciences, I. Ya. Postovskiy Institute of Organic Synthesis, 22 S. Kovalevskoy Street, Yekaterinburg 620219, Russian Federation
[d] Centre for Chemical Science and Technology, Institute of Science and Technology, Jawaharlal Nehru Technological University Hyderabad, Hyderabad 500085, Telangana, India
[e] Department of Biomedical Sciences and Therapeutics, Faculty of Medicine and Health Sciences, Universiti Malaysia Sabah, Kota Kinabalu 88400, Sabah, Malaysia
[f] Department of Biochemistry, Sri Venkateswara University College of Sciences, Sri Venkateswara University, Tirupati 517502, Andhra Pradesh, India
[g] Department of Chemistry, Sri Venkateswara University College of Sciences, Sri Venkateswara University, Tirupati 517502, Andhra Pradesh, India

ARTICLE INFO

Keywords:
α-Methyl-L-DOPA
Urea derivatives
Multiple molecular targets
Antioxidant activity
ADMET properties
Molecular docking studies

ABSTRACT

A series of novel α-methyl-L-DOPA urea derivatives *viz.*, 3-(3,4-dihydroxyphenyl)-2-methyl-2-(3-halo/trifluoromethyl substituted phenyl ureido)propanoic acids (**6a-e**) have been synthesized from the reaction of α-methyl-L-DOPA **(3)** with various aryl isocyanates **(4a-e)** by using triethylamine (**5**, TEA) as a base catalyst in THF at reflux conditions. The synthesized compounds are structurally characterized by spectral (IR, ^{1}H & ^{13}C NMR and MASS) and elemental analysis studies and screened for their *in-vitro* antioxidant activity against DPPH, NO and H_2O_2 free radical scavenging assays and identified compounds **6c** & **6d** as potential antioxidants. The acquired *in vitro* results were correlated with the results of molecular docking, ADMET, QSAR and bioactivity studies performed for them and predicted that the recorded *in silico* binding affinities are in good correlation with the *in vitro* antioxidant activity results. The molecular docking analysis has comprehended the strong hydrogen bonding interactions of **6a-e** with 1CB4, 1N8Q, 3MNG, 1OG5, 1DNU, 3NRZ, 2CDU, 1HD2 and 2HCK proteins of their respective SOD, LO, PRXS5, CP450, MP, XO, NO, PRY5 and HCK enzymes. This has sustained the effective binding of **6a-e** and resulted in functional inhibition of selective aminoacid residues to be pronounced as multiple molecular targets mediated antioxidant potent compounds. In addition, the evaluated toxicology risks of **6a-e** are identified with in the potential limits of drug candidates. The conformational analysis of **6c & 6d** prominently infers that urea moiety uniting α-methyl-L-DOPA with halo substituted aryl units into a distinctive orientation to comply good structure-activity to inhibit the proliferation of reactive oxygen species *in vivo*.

1. Introduction

In neurotherapy antioxidants are acknowledged as protective agents that efficiently works against the reactive oxygen species (ROS) to retard and to inhibit the aggregate effect of oxidative damages [1]. The renowned medical innovations evidences that the scarcity of antioxidants in brain causes neurological disorders like Parkinson's and Alzheimer's diseases, consequently fulfilled the etiology of such neurodegenerative diseases [2]. Oxidative stress realizes the pathogenesis of neurodegenerative diseases caused by the surplus amount of ROS produced *in vivo* by unbalanced biochemical disorders which intern leads to neuronal damage and cell death [3–6]. In this context, number of synthesized molecules varying in structures are under investigation for therapeutic use and many of them are getting agonized to cross the blood brain barrier (BBB) to warrant the activity. Hence, the identification of potential antioxidant active molecules with

* Correspondence author.
E-mail addresses: rajuchamarthi10@gmail.com (N.R. Chamarthi), pvchalapathisumathi@gmail.com (V.C. Ponne).

https://doi.org/10.1016/j.bioorg.2020.103708
Received 8 January 2020; Received in revised form 26 February 2020; Accepted 26 February 2020
Available online 29 February 2020

competent BBB threshold to pronounce as neuroprotective therapeutic agents is the significant task in current scenarios of biochemical research [7]. In such pursuit we have identified urea pharmacophore as privileged to present in some important medicines and drugs that are exhibiting both antioxidant and neuroprotective properties.

In this prominent array, 1-(2,6-dihalobenzoyl)-3-(9*H*-fluoren-9-yl)-urea **(I)** consisting an acyl urea moiety linking two aryl hydrophobic fragments is recognized as a Cyclophilin A (CypA) inhibitor [8] and reduces the neurological disorders in brain [9]. A novel class of 3-phenyl/ethyl-2-thioxo-2,3-dihydrothiazolo[4,5-*d*]pyrimidin-7-yl urea derivatives **(II)** have been identified as noteworthy anti-parkinsonian agents [10]. Similarly urea derivatives of quinoxaline 2,3-diones **(III)**, which are notorious glutamate receptor antagonists are identified as neuroprotective agents to treat chronic neurodegenerative disorders [11]. Alike 3-aroyl-1-(4-sulfamoylphenyl) urea derivatives **(IV)** containing aryl sulfonamide moiety are recognized as 15-lipoxygenase (15-LOX) inhibitors and potent antioxidants which works against oxidative stress induced cell death in PC12 cells by significant protection of neurons [12]. In continuation ethyl (benzo[*d*]thiazol-2-ylcarbamoyl) glycinate **(V)** a benzothiazole derivative an approved protecting agent of neuronal cells from amyloid β (Aβ25-35) induced apoptotic degeneration in PC12 cells [13]. Likely ethyl 6-methyl-4-(3-phenoxyphenyl)-2-thioxo-1,2,3,4-tetrahydro pyrimidine-5-carboxylate **(VI)**, a cyclic urea has potentially prohibited the neurotoxicity in N2a cells and identified as prospective neuroprotective agent and inhibited the inflammatory type of brain damage (Fig. 1) [14]. Indeed it is identified that urea pharmacophore is found to be potent with multi-ligating centers like oxygen and nitrogen atoms which acts as hydrogen bond donors to bind with the amino proton acceptors of the receptors and fulfills the drug properties. Hence these are identified as potent antimicrobial [15–23], anti-inflammatory [20], antioxidant [21–24], antidiabetic [19,25], antitubercular [17,26], antileishmanicidal [27] and anticancer [28,29] agents and 5-lipoxygenase [2], monoamine oxidase B [30], polyphenol oxidase [31], gastric H^+/K^+-ATPase [32], nitric oxide synthase [33] and urease [34] enzyme inhibitors.

Our proficiency in synthesis of urea derivatives having novel moieties *viz.*, 3-(trifluoromethyl)-5,6,7,8-tetrahydro-[1,2,4] triazolo [4,3-*a*] pyrazine, a newly designed drug intermediate containing both triazole and tetrahydropyrazine moieties [15], 2-amino-6-fluorochroman-2-yl) ethanol, a chromene based intermediate of Nebivolol drug [16], (2′-(1*H*-tetrazol-5-yl)biphenyl-4-yl)methanamine, a biphenyl moiety present in some drug intermediates like valsartan, A81988 and losartan [18] 2-amino-2,3-dihydro-1*H*-2λ^5[1,3,2]diazaphospholo[4,5-*b*] pyridin-2-one, a synthesized five membered diazaphosphole molecule [19] de-acidified AK-78710, a lopinavir drug intermediate comprising 2-oxotetrahydropyrimidin group [21], l-1-(3,4-Dihydroxyphenyl)-2-methylaminoethanol, a catechol substituted secondary amine [22], and 4-methyl-3-[4-(3-pyridyl)pyrimidin-2-ylamino]aniline, an imatinib drug intermediate [23] has significantly facilitated in refining the molecular design in connection with the structure activity relationship (SAR) studies that achieves the foreseen biological activity. Henceforth we have protracted our current investigative study to contemplate a new and potential moiety inhibiting the production of ROS to annihilate the oxidation process *in vivo* and also to acquire a potential threshold to cross BBB to have the eminence to be identified as neuroprotective antioxidants.

Here we have considered the renowned α-Methyl-L-DOPA [**3**, (*S*)-2-amino-3-(3,4-dihydroxyphenyl)-2-methylpropanoic acid] as a choice of potential excellence such that its basic structure represents many types of neurologically potent compounds. In this resembling series, (2*S*)-3-(3,4-dihydroxyphenyl)-2-hydrazino-2-methylpropanoic acid (Carbidopa, **VII**) is identified as potential inhibitor of aromatic L-amino acid decarboxylase (AADC) enzyme and it is identified as medication which is competent to passing through the protective blood–brain barrier (BBB) and is used in the treatment of Parkinson's disease (PD) [35]. Similarly (S)-6,7-dihydroxy-3-methyl-3,4-dihydroisoquinoline-3-carboxylic acid (**VIII**, 3-methyl derivative of 3,4-dihydroisoquinoline-3-carboxylic acid), which is derived from α-Methyl-L-DOPA is successfully identified as potential antioxidant and D-aminoacid oxidase (DAAO) inhibitor and reported as useful compound for the treatment of neurodegenerative diseases [36]. In this context, (4*S*)-1-chloro-7,8-dihydroxy-4-methyl-2-oxo-1,4,5,9*b*-tetrahydro-2*H*-azeto[2,1-*a*]isoquinoline-4-carboxylic acid (**IX**, a β-lactam derivative of 3,4-dihydroisoquinoline-3-carboxylic acid), which is derived from α-Methyl-L-DOPA is recognized as a potential compound that inhibit the growth of butyrylcholinesterase (BuChE) and acetylcholinesterase (AChE) enzymes that effectively works for pathophysiology of Alzheimer's disease [36]. In hierarchy, 1-(pivaloyloxy)ethyl (2*S*)-2-amino-3-(3,4-dihydroxyphenyl)-2-methylpropanoate (**X**, pivaloyloxyethyl ester of methyldopa) is identified as a potential antihypertensive agent playing an important role in neurotransmission [37].

Additionally, it is predicted that (R)-2-(((R)-1-carboxy-3-oxo-3-phenylpropyl)-L-alanyl)-6,7-dimethoxy-3-methyl-1,2,3,4-tetrahydroisoquinoline-3-carboxylic acid (**XI**, 3-Phenyl moexiprilat), which is derived from α-Methyl-L-DOPA is identified as proficient lipophilic angiotensin converting enzyme (ACE) inhibitors and controls the arterial hypertension [38,39]. Furthermore, ethyl (R)-2-((3S,11aS)-8,9-dimethoxy-3,11a-dimethyl-1,4-dioxo-1,3,4,6,11,11a-hexahydro-2H-pyrazino[1,2-b]isoquinolin-2-yl)-4-oxo-4-phenylbutanoate (**XII**, diketopiperazine derivative of 3-Phenyl moexiprilat), which is derived from α-Methyl-L-DOPA is also described as active angiotensin-converting enzyme (ACE) inhibitor (Fig. 1) [40]. Apart from these neurological applications of α-methyl-L-DOPA derivatives, they have been also reported as ultimate antihypertensive agent [41], anti-parkinson's drug [42], sympathetic nerve inhibitor that reduces the blood pressure by inhibiting the sympathetic nerves from compressing blood vessels [43] human L-type amino acid transporter 1 (LAT1) endogenous candidate that regulates the its high level of consistent expression in brain microvessel endothelial cells and acts as therapeutic neuropharmaceutical agent [44,45]. Hence, we have designed the synthesis of a series of α-methyl-L-DOPA urea derivatives, synthesized, studied and herein reporting as potential antioxidants those outrivals the potential BBB threshold to be quantified as neuroprotective antioxidants and rewarded the present study.

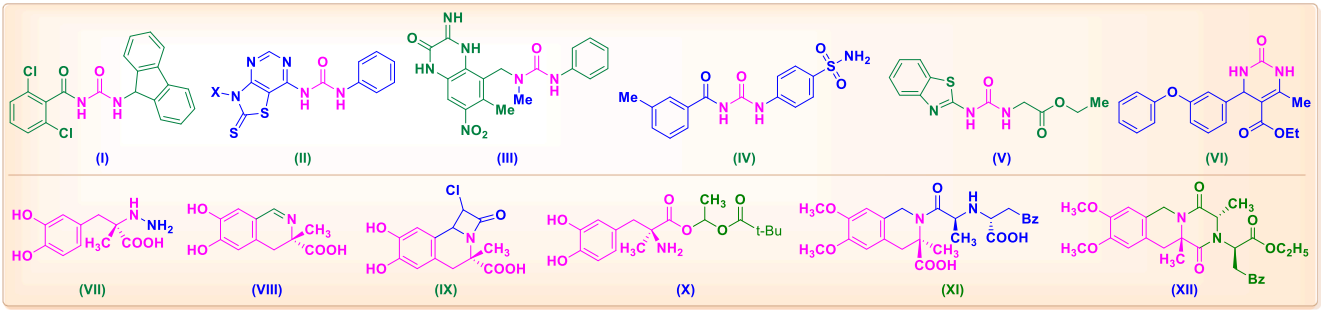

Fig. 1. Neuro-Potent urea derivatives **(I-VI)** & α-methyl-L-DOPA derivatives **(VII-XII)**.

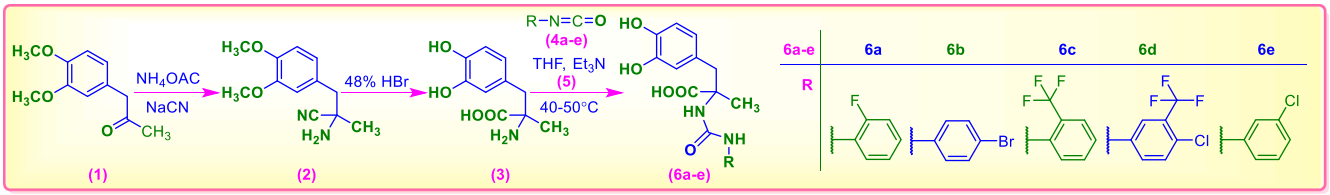

Scheme 1. Synthesis of urea derivatives of α- methyl- L-Dopa (6a-e).

2. Results and discussion

2.1. Chemistry

3-(3,4-dihydroxyphenyl)-2-methyl-2-(3-halo/trifluoromethyl substituted phenyl ureido)propanoic acids (**6a-e**) have been synthesized from the reaction of α-methyl-L-Dopa (**3**), phenyl isocyanates (**4a-e**) and TEA (**5**) base (Scheme 1). The merit of this reaction is easy work-up to obtain products in good yields with the optimized conditions of TEA base and THF solvents.

2.1.1. Optimization of base catalyst for the reaction

Compound **3** was taken in to a round bottom flask containing *o*-fluorophenyl isocyanate in THF in sodium hydroxide base and thoroughly stirred the contents for 8 h at 40–50 °C and poor result was observed. Then the same reaction was performed by varying sodium hydroxide with potassium hydroxide, cesium carbonate, potassium hydroxide & ammonia and obtained the same result. Then used L-proline, *N*,*N*-diethylamine and triethylamine and obtained significantly higher yields. Hence we shifted to engage reaction with organc bases like triphenyl phosphine, pyridine, pyrrolidine, *di-iso*propyl ethyl amine, *p*-toluenesulfonic acid and observed no considerable progress in the yield. In ultimate, highest yield was obtained with TEA base (Table 1) and thus noted it as a base catalyst of interest for the synthesis of **6a-e** and same conditions were adopted for the solvent optimization.

2.1.2. Optimization of solvent for the reaction

After optimizing TEA as an efficient catalyst for the synthesis of title compounds, we have screened various solvents same conditions apart THF. In such we have engaged some polar protic solvents like ethanol, isopropyl alcohol & methanol, polar aprotic solvents like acetonitrile, 1,2-dichloromethane, dimethyl sulfoxide, *N*,*N*-dimethylformamide, 1,2-dichloroethane and non-polar solvents like 1,4-dioxane, chloroform, *o*-xylene & toluene and performed the reaction at 40–50 °C for 8 h (Table 2). From the results it is identified that THF system has given 90% yield and no other solvent has been successful and hence we have considered THF as an effective solvent and moved for the synthesis of remaining compounds of the series in good yields.

Table 1
Optimization of base for the synthesis of **6a**.

S.No.	Catalyst[a,b]	Yield (%)[c,d]
1	Sodium hydride	10
2	Potassium carbonate	10
3	Cesium carbonate	20
4	Potassium hydroxide	Nil
5	Ammonia	Nil
6	L-Proline	30
7	*N*,*N*-Diethylamine	30
8	Triethylamine	90
9	Triphenyl phosphine	20
10	Di-*iso*propyl ethyl amine	40
11	*p*-Toluenesulfonic acid	10
12	Pyridine	20
13	Pyrrolidine	10

[a] Solvent: Tetrahydrofuran (THF).
[b] Catalyst Concentration: 20 mol%.
[c] Reaction temperature: 45–50 °C.
[d] Reaction time: 8 h.

Table 2
Optimization of solvent for the synthesis of **6a**.[a–d]

S.No.	Solvent	Yield (%)
1	Methanol	50
2	Ethanol	50
3	Isopropyl alcohol (IPA)	40
4	1,2-Dichloromethane (DCM)	40
5	1,2-Dichloroethane	45
6	Acetonitrile	35
7	*N*,*N*-Dimethylformamide	30
8	Dimethyl sulfoxide (DMSO)	30
9	Tetrahydrofuran (THF)	90
10	Chloroform	50
11	1,4-Dioxane	Nil
12	Toluene	Nil
13	*o*-Xylene	Nil

[a] Catalyst: Triethylamine (TEA).
[b] Catalyst concentration: 20 mol%.
[c] Reaction temperature: 45–50 °C.
[d] Reaction time: 8 h.

2.1.3. Mechanism for the synthesis of compounds *6a-e*

Here the base action of TEA has been clearly visualized in obtaining title compounds from substrates (Fig. 2). At the outset, TEA base (**5**, pk_a: 10.78) abstracts a proton from α-methyl-L-DOPA (**3**, pk_a: 9.85) and produces its conjugate acid (**7**, triethylammonium ion, pk_a: 10.75) along with (2-carboxy-1-(3,4-dihydroxyphenyl)propan-2-yl)amide anion (**8**). Then **8** acts as a base and attacks on isocyanate's caronyl carbon (electrophilic) of aryl isocyanate (**4**), generates ((2-carboxy-1-(3,4-dihydroxy phenyl)propan-2-yl)carbamoyl)(phenyl)amide anion **(9)** in addition reaction approach. In ultimate, intermediate anion **9** abstracts a proton from triethylammonium ion (**7**), and forms 3-(3,4-dihydroxyphenyl)-2-methyl-2-(3-halo/trifluoro-methyl substituted phenyl ureido)propanoic acids **(6a-e)**. The reaction is well expedited in THF, as it is unable to strongly bound with the intermediates and title compounds and accelerates the reaction to accomplish the **6a-e** in good yields with short reaction times.

2.2. Antioxidant activity

Pioneering of potential antioxidants is a significant objective as that one may to remove surplus free radicals *in vivo*. In this pursuit, we have prospered α-Methyl-L-DOPA, customized its structure by introducing some aryl groups with a urea spacer. The screened DPPH assay results customized compounds **6a-e** with 17.13–20.44 μM range of Half Maximal Inhibitory Concentration (IC_{50}), **3** with 183.68 μM, ascorbic acid with 16.05 μM and **6c** with 17.13 μM (Table 3). Similarly the screened NO assay results customized compounds **6a-e** with 95.05–101.72 μM range of IC_{50}, **3** with 109.38 μM, ascorbic acid with 47.84 μM and **6c** with 95.05 μM (Table 4). In addition, screened H_2O_2 assay results customized compounds **6a-e** with 22.11–100.90 μM range of IC_{50}, **3** with 109.38 μM, ascorbic acid with 20.47 μM and **6c** with 22.11 μM (Table 5). The obtained results customized **6a-e** in an order of **6c** > **6d** > **6e** > **6b** > **6a** potential antioxidant activity. Finally,

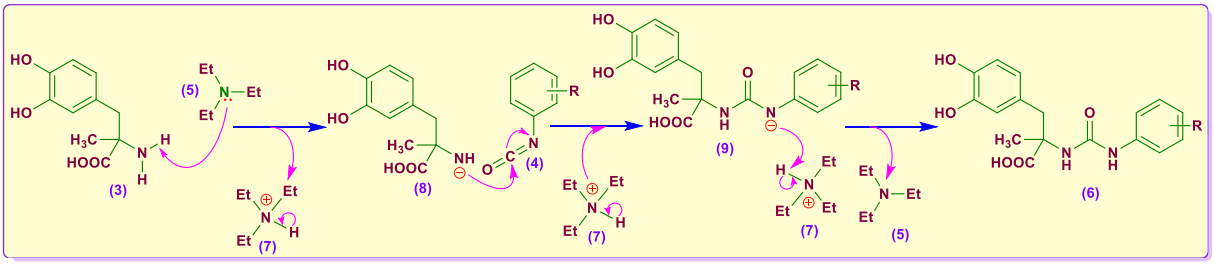

Fig. 2. Mechanism for the synthesis of compounds **6a-e.**

compound **6c** is identified as potential antioxidant as it is emphasized with consistent results in three *in vivo* assays we studied. In ultimate the idea of intriguing aryl moieties with urea spacer on amino group of *α*-Methyl-*L*-DOPA to fascinate antioxidant activity is fulfilled.

2.3. Molecular docking studies:

The inhibition of proliferation of ROS *in vivo* by **6a-e** has been mechanistically assessed by interpreting their molecular docking interactions with selective enzymatic proteins *viz.*, 1CB4 (superoxide dismutase) [46], 1N8Q (Lipoxygenase-3) [47], 3MNG (Peroxiredoxin-5) [48], 1OG5 Cytochrome p450 [49], 1DNU (Myeloperoxidase) [50], 3NRZ (Xanthine dehydrogenase/oxidase) [51], 2CDU (NADPH oxidase) [52], 1HD2 (Peroxiredoxin 5) [53] and 2HCK (Hematopoetic cell kinase) [54] and studied the ligand-protein binding patterns. The docking interactions of selective aminoacid residues with hydrogen bond donor and acceptor atoms of title compounds **(**Table 6, 8, 10, 12 & 14**)** and their docking poses of protein-ligand interactions **(**Tables 7, 9, 11, 13 & 15**)** were presented. In detail, the conformational analysis of **6a-e** confirms that carboxylic and di-hydroxyphenyl groups (in planes) are linked by C_{α}–C_{β} bond with an angle of 179.8–180.0°, resembling methyl-DOPA. Similarly, C_{α}–CH_3 & C_{Ar}–CF_3 groups linked by urea (–N-H–CO–NH–) are with inter planar angle of 179.5–179.8° **(**Fig. 3**)**. It is also predicted that both $-CF_3$ & $-CH_3$ moieties have oriented in trans geometry and adopted an virtual octahedral (all counter corner atoms are ~4A° apart) orientation which are 5A°apart. In wholesome the presence of classical and nonpolar methyl isosteric trifluoromethyl ($-CF_3$) moiety in compounds **6c** and **6d** has attributed high potentiality and the its unique structure-bioactivity analogy as $-CF_3$ moiety is located far away from the *α*-carbon of these compounds rather than to disturb the inherent properties [55].

2.4. ADMET properties:

Study of ADMET properties for an ensemble of compounds helps to understand and describe their physico-chemical interactions with target and assists us to assess its drug like properties and helps a lot in drug design and development. This high-throughput screening of molecular adherence helps in recognizing a lead compound of a large ensemble in the interested targets domain [56].

This significant study helps to distinguish the pharmacokinetic properties of **6a-e** and to comprehend their drug-like interactions with in the cell. The Human intestinal absorption discursively helps in carrying the active compounds to target cell tissues *via* blood stream to interact mutually. In oral administration, degree of absorption of a potential compound depends on the properties of its inherent bioavailability. Then the absorbed portion will itself be distributed into muscles from there to other organs by circulation *via* extracellular sites. As such the distribution of a compound lowers its plasma concentration and metabolizes it and then distributes its metabolites by enzymatic redox reactions. Some of the distributed active metabolites work efficiently in pharmacologically on cellular systems, on contrary the inactive metabolites deactivate the administered compound and reduce its effect *in vivo* and inert metabolites will be excreted from kidneys.

The scrutiny of predicted ADMET properties (Table 16) of **6a-e** revealed that the *in vivo* BBB penetration efficiency identified in the range of 0.294438–0.749112 ascertains their high significance of CNS activity approved their permeability to distribute themselves *in vivo* compared to substrate **3** with 0.472612 and ascorbic acid with 0.172436. It is reinforced on the grounds of their *in vitro* Caco-2 cell permeability observed in the range of 18.8199–21.0311 nm/sec, which are benign compared to the substrate **3** with 21.1075 and ascorbic acid with 2.65695. This efficiency establishes their sustained permeability to bind with the plasma proteins to enable the penetration of these compounds in to BBB system. The *in vitro* PPB affinity observed in the range of 82.476035–92.817459% confirms their strong binding ability to the plasma proteins, which are worthy, compared to the substrate **3** with 9.079006 and ascorbic acid with 2.790093. The *in vitro* MDCK cell permeability acknowledged in the range of 0.031757–2.42001 nm/sec and hence discloses them as moderately permeable to interact with the concerned active species, compared to the substrate **3** with 14.7944 and ascorbic acid with 0.72561. The %HIA recognized is proficient as they are in the range of 77.637382–86.697345 which are comparatively better than compound **3** with 61.912798% and standard ascorbic acid with 29.075921% and promises their interactions with the reactive species in the expecting target of domains. The negative toxicity results indicate that compounds **6a-e** are safer and non-toxic drugs as omitted from the positive toxicity results. This study concludes the good physico-chemical interactions of **6a-e** and their drug-likeness properties.

Table 3
DPPH free radical scavenging activity of **6a-e.**

Compound	Percentage of Scavenging (%)				Half Maximal Inhibitory Concentration (IC_{50} in μM)
	25 μg/mL	50 μg/mL	75 μg/mL	100 μg/mL	
6a	61.15 ± 0.28	64.62 ± 0.31	66.94 ± 0.13	69.25 ± 0.22	20.44
6b	63.47 ± 0.21	66.94 ± 0.27	67.4 ± 0.15	69.95 ± 0.33	19.69
6c	72.96 ± 0.32	73.19 ± 0.24	74.02 ± 0.16	78.05 ± 0.12	17.13
6d	65.20 ± 0.20	67.87 ± 0.16	69.72 ± 0.24	71.57 ± 0.28	19.17
6e	63.93 ± 0.18	68.33 ± 0.40	70.64 ± 0.18	72.26 ± 0.46	19.55
3	11.07 ± 0.94	15.54 ± 0.52	22.35 ± 0.57	29.67 ± 0.35	183.68
Ascorbic Acid	77.84 ± 0.21	78.04 ± 0.11	81.01 ± 033	84.02 ± 0.47	16.05

Table 4
NO free radical scavenging activity of **6a-e.**

Compound	Percentage of Scavenging (%)				Half Maximal Inhibitory Concentration (IC_{50} in μM)
	25 μg/mL	50 μg/mL	75 μg/mL	100 μg/mL	
6a	30.52 ± 0.38	36.42 ± 0.23	43.12 ± 0.43	49.15 ± 0.32	101.72
6b	33.32 ± 0.11	39.4 ± 0.17	47.9 ± 0.35	50.45 ± 0.13	99.10
6c	35.25 ± 0.45	39.36 ± 0.82	45.8 ± 0.44	52.6 ± 0.22	95.05
6d	32.54 ± 0.60	39.46 ± 0.36	46.42 ± 0.18	51.27 ± 0.10	97.52
6e	30.06 ± 0.15	35.4 ± 0.26	45.8 ± 0.63	55.7 ± 0.38	98.70
3	25.37 ± 1.35	28.44 ± 1.19	37.81 ± 0.96	48.75 ± 1.11	109.38
Ascorbic Acid	40.11 ± 0.62	52.25 ± 0.32	61.66 ± 0.09	69.23 ± 0.32	47.84

2.5. QSAR studies

The study of biochemical interactions of compound under analysis with it pharmacological target is a vital step in realizing its drug-like properties. In such predicted QSAR properties of **6a-e** revealed their effective scorings of molecular weights are in 364.79–432.78 range, which are less than 500 Da and supports their safer drug activity (Table 17). The number of hydrogen bond donating atoms or atom containing groups is 5, which is less than or equal to 5, basically, the urea moiety is a powerful hydrogen bond donor [57,58] and the number of hydrogen bond accepting atoms or atom containing groups is 6, which is less than 10. Similarly, they are deserved with partition coefficient (logP) of 1.81–3.17, which is less than 5 and the molecular refractivity values in the range of 87.79–97.67 cm^3/mol are identified in the limits of potential drugs only. These observed results confirm that compounds **6a-e** are with virtuous pharmaceutical parameters with zero Lipinski property violations. On compatible with Lipinski parameters we have predicted the total polar surface area (TPSA) value as 118.88 which is less than 140, number of rotatable bonds in the range of 5–6 which are less than 10 empowers them as potential molecules with zero Veber property violations to interact well with the target cells. The consistent correlation of Lipinski and Veber properties esteems compound **6a-e** as noble administrable drugs to effectively bind with host to assure their pharmacological activity.

On the other hand, the number of hydrophobic atoms presents on the ligand molecules in the range of 17–18 assures their capacity to form complexes with target cell receptors to institute their ligand-receptor binding relations. The additional properties like Van der Waals volume identified in the range of 237.2–278.5, density in the range of 1.467–1.641gm/cc and solubility ranging from −3.26 to −4.46 supports the of ligand interactions with molecules with the hosting receptors and their proficient affinity with target cells within binding domain. This entire study of QSAR properties of **6a-e** concludes their established structure-activity relationship parameters to support the evaluated antioxidant potentiality and to state them as neuro-protective antioxidants.

2.6. Bioactivity & toxicity risk studies

The bioactivity properties like G protein-coupled receptor Ligand (GPCRL) property, ion channel modulator (ICM) property, kinase inhibitor (KI) property, protease inhibitor (PI) property, nuclear receptor ligand (NRL) interaction property & enzyme inhibitor (EI) property and toxicity risk properties like drug-likeness and drug score were predicted for the title compounds (Table 18). The GPCRL property is identified in the limits of 0.22–0.31, ICM property is identified ranging from −0.03 to 0.10, KI property is identified limiting from −0.08 to 0.01, NRL interaction property is enriched **6a-e** with values ranging from −0.16 to 0.09, PI property is reputed in the range of 0.31–0.19 and EI property is explored in the limits of 0.03–0.09. All these properties are superior to the compared standards and the substrate *α*-methyl-*L*-DOPA. Similarly, it is found that all the compounds are in the range of −8.78 to 0.48 of drug-likeness and is comparable with ascorbic acid standards having −6.5 of drug-likeness. Likewise, the drug score is identified in the range of 0.27 to 0.64, which are analogous to the ascorbic acid standard with 0.49 of drug score value. From the bioactivity assessment, it is also renowned that all the synthesized compounds are non-mutagenic, non-tumorigenic, non-irritant and they doesn't adhere the negative impacts on reproductive system and hence ascertained them as safer drugs with extensive binding affinities to pair up potentially with reactive species in the domains of the specific targets considered and established a robust host-receptor relation of compounds **6a-e** with the all the above ligands.

3. Conclusion

A series of novel *α*-methyl-*L*-DOPA urea derivatives *viz.*, 3-(3,4-dihydroxyphenyl)-2-methyl-2-(3-halo/trifluoromethyl substituted phenyl ureido)propanoic acids **(6a-e)** synthesized by using TEA base as it assisted the reactants to bind and form C—N bond *via* addition reaction. Here, **6c** & **6d** were identified as effective antioxidants with good IC_{50} values as screened at 25, 50, 75 and 100 μg/mL assessed by DPPH, NO & H_2O_2 scavenging methods. Their molecular docking studies, ADMET, QSAR, toxicity risks and bioactivity studies have reinforced their drug-likeness, correlated with *in vivo* antioxidant activity. In addition, the neuroprotective property has been arbitrated with BBB penetration

Table 5
H_2O_2 free radical scavenging activity of **6a-e.**

Compound	Percentage of Scavenging (%)				Half Maximal Inhibitory Concentration (IC_{50} in μM)
	25 μg/mL	50 μg/mL	75 μg/mL	100 μg/mL	
6a	41.51 ± 0.28	44.22 ± 0.31	46.14 ± 0.13	49.55 ± 0.22	100.90
6b	42.16 ± 0.33	45.45 ± 0.24	50.6 ± 0.19	54.4 ± 0.22	74.11
6c	56.52 ± 0.23	63.27 ± 0.36	74.10 ± 0.24	82.12 ± 0.42	22.11
6d	48.16 ± 0.65	57.64 ± 0.16	68.9 ± 0.54	83.4 ± 0.32	25.95
6e	45.10 ± 0.40	49.76 ± 0.66	56.72 ± 0.14	61.47 ± 0.08	50.24
3	25.37 ± 1.35	28.44 ± 1.19	37.81 ± 0.96	48.75 ± 1.11	109.38
Ascorbic Acid	61.06 ± 0.55	67.22 ± 0.22	74.04 ± 0.02	84.96 ± 0.33	20.47

Table 6
Molecular Docking interactions of compound **6a** with identified enzymatic proteins.

Enzymatic Protein	Cluster Number	Cluster Rank	Binding Energy (KCal/mol)	No. of Hydrogen Bonds	H-Bond Ligand Atoms	H-Bond Receptor Atoms	Binding interaction	Bond Length (A°)	H-Bond Type
1CB4 Chain A of Superoxide Dismutase (SOD)	0	0	−7.6935	5	4	3	Ligand(NH)——————————ASP25(O)	2.512	Acceptor
							Ligand(N'H)——————————ASP25(O)	2.350	Acceptor
							Ligand(OH)——————————GLU107(O)	1.827	Acceptor
							Ligand(OH)——————————GLU107(O)	1.794	Acceptor
							Ligand(NH)——————————PRO100(O)	1.2411	Acceptor
1N8Q Chain A of Lipoxygenase-3 (LO)	3	1	−8.6670	4	4	4	Ligand(OH)——————————ASP787(O)	1.733	Acceptor
							Ligand(HO)——————————ASN788(NH)	2.201	Donor
							Ligand(HN-C═O)–ASN146(NH)	2.485	Donor
							Ligand(COOH)——————VAL539(O)	1.688	Acceptor
3MNG Chain A of Peroxiredoxin-5 (PRX5)	2	0	−7.9323	5	5	4	Ligand(NH)——————————PRO100(O)	1.877	Acceptor
							Ligand(N'H)——————————PRO100(O)	2.498	Acceptor
							Ligand(HO)——————————ASN122(NH)	2.353	Donor
							Ligand(C═O)————ASN122(NH')	2.433	Donor
							Ligand(OH')————ASP77(COOH)	2.124	Acceptor
1OG5 Chain B of Cytochrome P450 (CP450) - 2C9	20	0	−8.1564	3	3	2	Ligand(HO)——————————PHE476(NH)	2.541	Donor
							Ligand(OH)——————————ASN474(O)	2.743	Acceptor
							Ligand(OH')——————————ASN474(O)	2.099	Acceptor
1DNU Chain C of Myeloperoxidase (MP)	0	3	−8.3766	2	2	2	Ligand(OH)——————————GLU242(O)	2.212	Acceptor
							Ligand(H'O)——————ARG239(NH)	2.349	Donor
3NRZ Chain L of Xanthine Oxidase (XO)	41	0	−8.4701	3	2	3	Ligand(OH)——————————SER1080(O)	2.479	Acceptor
							Ligand(HO)——————————PHE798(NH)	2.289	Donor
							Ligand(HO)——————————GLY797(NH)	2.512	Donor
2CDU Chain B of NADPH Oxidase (NO)	0	0	−8.3735	2	2	2	Ligand(COOH)–GLU32(COOH)	1.836	Acceptor
							Ligand(HN-C═O)–LYS134(NH)	2.581	Donor
1HD2 Chain A of Peroxiredoxin-5 (PRY5) Residue (54-214)	2	0	−7.9280	3	3	3	Ligand(HOC = O)————LEU96(NH)	1.913	Donor
							Ligand(COOH)——————VAL94(O)	1.980	Acceptor
							Ligand(HN-C═O)—ARG86(NH)	2.020	Donor
2HCK Chain B of Hematopoetic Cell Kinase (HCK)	0	3	−7.7634	4	3	3	Ligand(NH)——————————GLN161(CO)	2.144	Acceptor
							Ligand(NH')——————————GLN161(CO)	1.956	Acceptor
							Ligand(COOH)–ASP320(COOH)	2.108	Donor
							Ligand(COOH)–ASP320(COOH)	1.888	Donor

Table 7
Potential protein-ligand binding interactions of compound **6a** with identified enzymatic proteins.

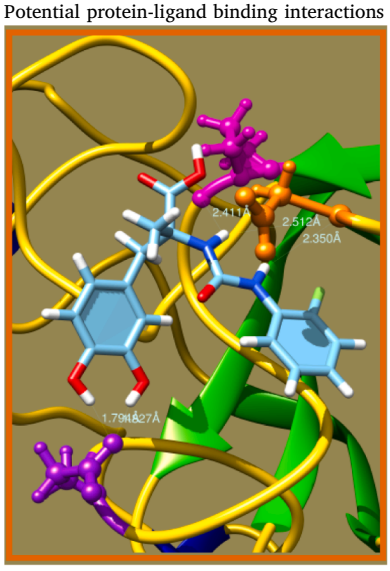

6a with 1CB4 Chain A of SOD Enzyme

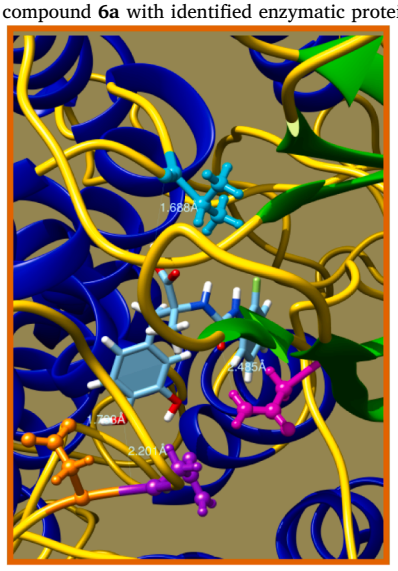

6a with 1N8Q Chain A of LO Enzyme

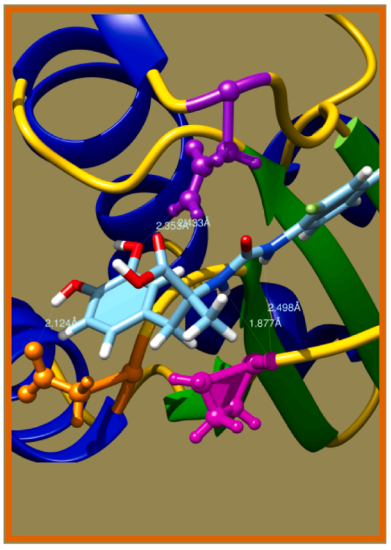

6a with 3MNG Chain A of PRXS5 Enzyme

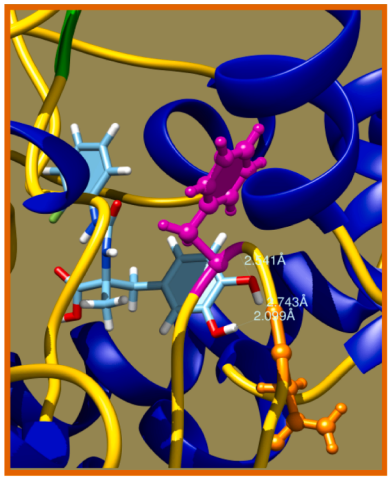

6a with 1OG5 Chain B of CP450 Enzyme

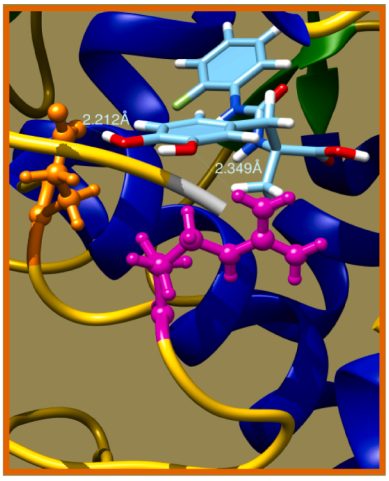

6a with 1DNU Chain C of MP Enzyme

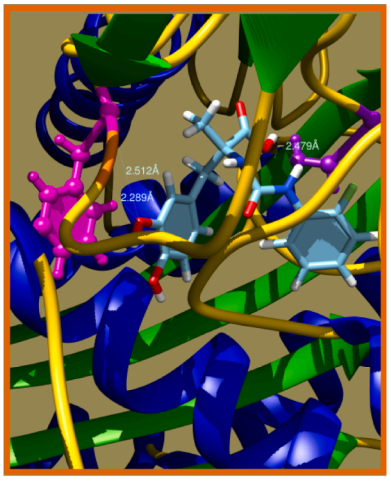

6a with 3NRZ Chain L of XO Enzyme

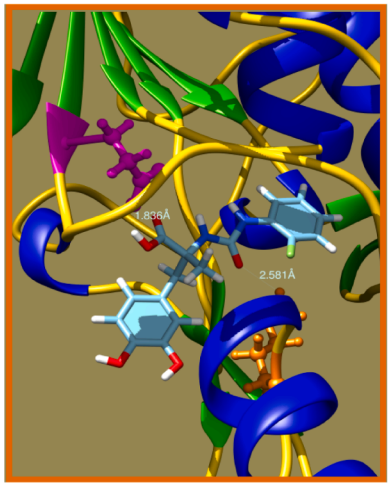

6a with 2CDU Chain B of NO Enzyme

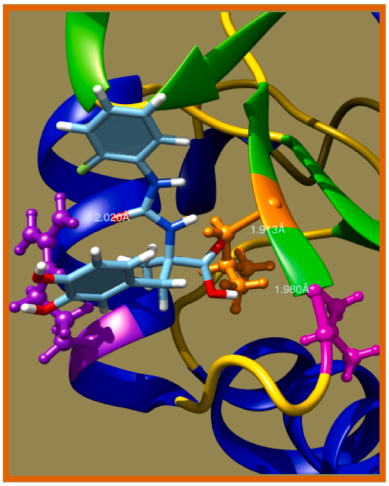

6a with 1HD2 Chain A of PRY5 Enzyme

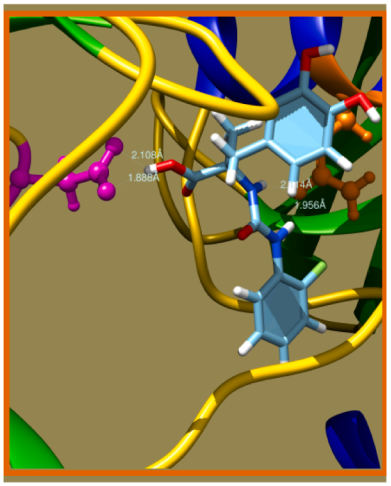

6a with 2HCK Chain B of HCK Enzyme

studies as they easily surpass the BBB threshold with good penetration rates. This prediction has endorsed them as CNS active neuro-protective antioxidants as preceded with the LAT1 transporter conjugate ability of parent *α*-methyl-*L*-DOPA. As **6a-e** binds with proteins 1CB4 (Chain A) of superoxide dismutase (SOD), 1N8Q (Chain A) of lipoxygenase-3 (LO), 3MNG (Chain A) of peroxiredoxin-5 (PRXS5), 1OG5 (Chain B) of cytochrome p450 (CP450), 1DNU (Chain C) of myeloperoxidase (MP), 3NRZ (Chain L) of xanthine dehydrogenase/oxidase (XO), 2CDU (Chain

Table 8
Molecular Docking interactions of compound **6b** with identified enzymatic proteins.

Enzymatic Protein	Cluster Number	Cluster Rank	Binding Energy (KCal/mol)	No. of Hydrogen Bonds	H-Bond Ligand Atoms	H-Bond Receptor Atoms	Binding interaction	Bond Length (A°)	H-Bond Type
1CB4 Chain A of Superoxide Dismutase (SOD)	0	1	−7.6831	5	4	3	Ligand(NH′)———— PRO100(O)	2.734	Acceptor
							Ligand(NH)———— PRO100(O)	1.863	Acceptor
							Ligand(OH)———— GLU107(O)	1.932	Acceptor
							Ligand(OH′)————GLU107(O)	1.780	Acceptor
							Ligand(NH)———— ASP25(O)	2.396	Acceptor
1N8Q Chain A of Lipoxygenase-3 (LO)	6	0	−9.0584	4	4	4	Ligand(OH)———— ASP787(O)	1.724	Acceptor
							Ligand(HO)————ASN788(NH)	2.231	Donor
							Ligand(HN-C═O)–ASN146(NH)	2.465	Donor
							Ligand(COOH)————VAL539(O)	1.816	Acceptor
3MNG Chain A of Peroxiredoxin-5 (PRX5)	25	3	−7.6723	3	3	3	Ligand(OH)————GLU91(OCOH)	2.039	Acceptor
							Ligand(HOCO)————LEU96(NH)	1.864	Donor
							Ligand(CONH′)————VAL94(O)	2.353	Acceptor
1OG5 Chain B of Cytochrome P450 (CP450) - 2C9	19	4	−7.8594	3	3	3	Ligand(CONH)————LEU208(O)	2.696	Acceptor
							Ligand(HOCO)———PHE476(NH)	2.080	Donor
							Ligand(COOH)————ASN474(O)	1.722	Acceptor
1DNU Chain C of Myeloperoxidase (MP)	2	2	−8.5266	3	3	3	Ligand(OH)———— GLU242(O)	2.405	Acceptor
							Ligand(H′O)————ARG239(NH)	2.231	Donor
							Ligand(COOH)————ASP237(O)	2.586	Acceptor
3NRZ Chain L of Xanthine Oxidase (XO)	7	1	−8.9480	4	4	4	Ligand(OH)–GLN1194(OCNH)	2.031	Acceptor
							Ligand(HO)—GLN1194(HNCO)	2.318	Donor
							Ligand(CONH)———THR1077(O)	2.455	Acceptor
							Ligand(HNCO)–GLN1040(CONH)	2.939	Donor
2CDU Chain B of NADPH Oxidase (NO)	1	0	−8.9611	6	4	6	Ligand(HOCO)—ASN135(HNCO)	2.136	Donor
							Ligand(HOCO)–ASN34(HNCO)	2.234	Donor
							Ligand(CONH′)–GLU32(COOH)	2.353	Acceptor
							Ligand(CONH′)–GLU32(COOH)	2.434	Acceptor
							Ligand(H′O)————ALA11 (NH)	2.092	Acceptor
							Ligand(HO)————THR9(NH)	2.293	Acceptor
1HD2 Chain A of Peroxiredoxin-5 (PRY5) Residue (54-214)	8	1	−7.8723	4	3	4	Ligand(COOH)————LEU96(O)	2.429	Acceptor
							Ligand(HOC = O)————LEU96(NH)	2.031	Donor
							Ligand(HN-C═O)——ARG86(NH)	2.051	Donor
							Ligand(HN-C═O)——ARG86(NH)	2.659	Donor
2HCK Chain B of Hematopoetic Cell Kinase (HCK)	10	7	−8.1787	6	5	6	Ligand(COOH)—ASP348(COOH)	2.101	Acceptor
							Ligand(HOCO)———SER345(OH)	2.509	Acceptor
							Ligand(HOCO)———SER345(NH)	1.945	Acceptor
							Ligand(OH)———— MET341(O)	2.554	Acceptor
							Ligand(HO)———— MET341(HN)	2.541	Donor
							Ligand(CONH′)————ALA275(O)	1.888	Acceptor

B) of NADPH oxidase (NO), 1HD2 (Chain A) of peroxiredoxin 5 (PRY5) and 2HCK (Chain B) of hematopoetic cell kinase (HCK) enzymes with strong hydrogen bond binding affinities (ranging from −7.3359 to −9.111 KCal/mol), to inhibit the ROS produced during metabolism and their inhibitions break the ROS production by ensuing the reduction of the oxidative species and conservation of redox homeostasis.

Remarkably title compounds are identified to bound with aminoacids in the order of their decreasing number of interactions with the ligands *viz.*, aspartic acid (ASP), glutamic acid (GLU) and asparagine (ASN), arginine (ARG), threonine (THR), valine (VAL), phenyl alanine (PHE), serine (SER), leucine (LEU), glutamine (GLU), alanine (ALA), methionine (MET), proline (PRO), glycine (GLY), lysine (LYS), histidine (HIS), cysteine (CYS) and tyrosine (TYR). The profound investigation reveals that acidic aminoacids are strongly bound to the ligands rather than neutral and basic aminoacids. This clearly reveals the carboxylic acid extended interaction of enzymatic proteins with amino ends of urea moiety present in the title compounds. Such that the prominence of multiple molecular targets mediated antioxidant activity of **6a-e** has been well justified with potential excitatory protein receptor antagonist enactment to reduce and block the neuronal damages and death, positively treat the neuro-degenenerative disorders. Hence, the idea of linking *α*-methyl-*L*-DOPA and halo substituted aryl moieties with urea linker has been proved as a commending assignment in designing these potential antioxidants and proved *α*-methyl-*L*-DOPA group as potential pharmacophore of the synthesized halo substituted urea derivatives.

4. Materials & methods

4.1. Chemistry

Chemicals were procured from Merck, progress of reaction was monitored by thin layer chromatography (TLC, Merck) plates by observing in UV (ultraviolet) lamp light (Hyderabad, India) and iodine by absorbance. Synthesized compounds were obtained in pure form by column chromatography (silica gel 200–300) and mp (melting points) were determined on MP490 digital melting point apparatus (Hyderabad, India) in open

Table 9
Potential protein-ligand binding interactions of compound **6b** with identified enzymatic proteins.

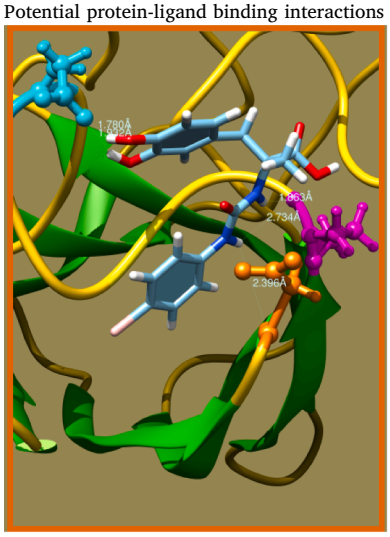

6b with 1CB4 Chain A of SOD Enzyme

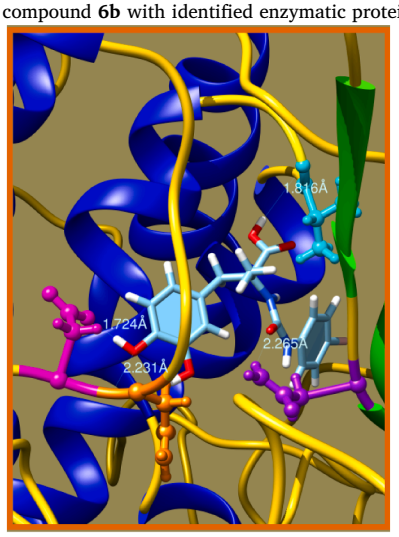

6b with 1N8Q Chain A of LO Enzyme

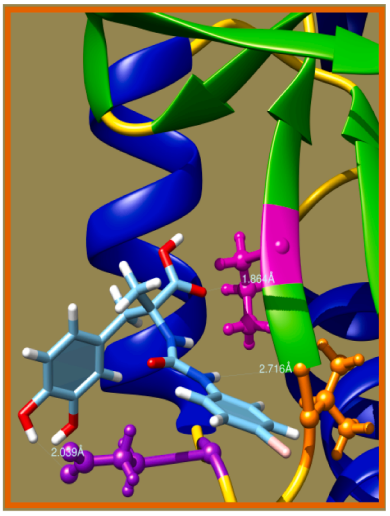

6b with 3MNG Chain A of PRXS5 Enzyme

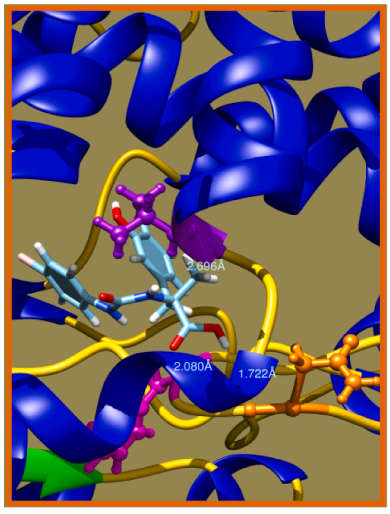

6b with 1OG5 Chain B of CP450 Enzyme

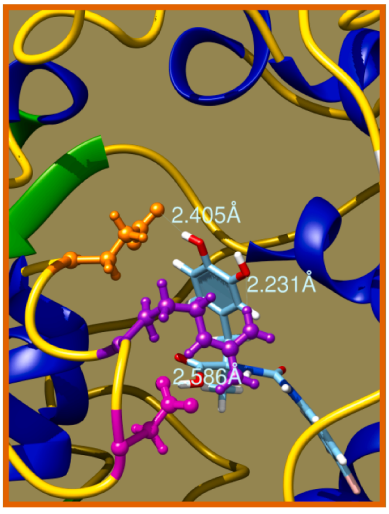

6b with 1DNU Chain C of MP Enzyme

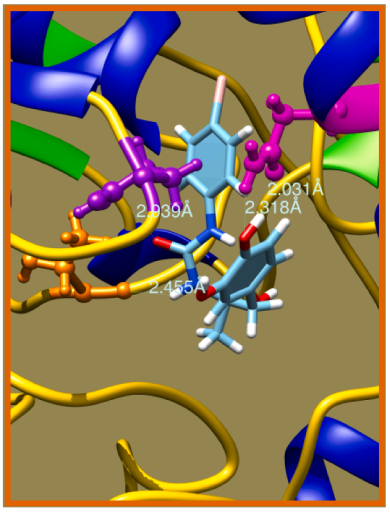

6b with 3NRZ Chain L of XO Enzyme

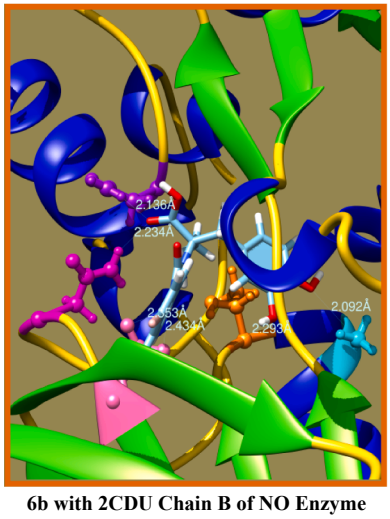

6b with 2CDU Chain B of NO Enzyme

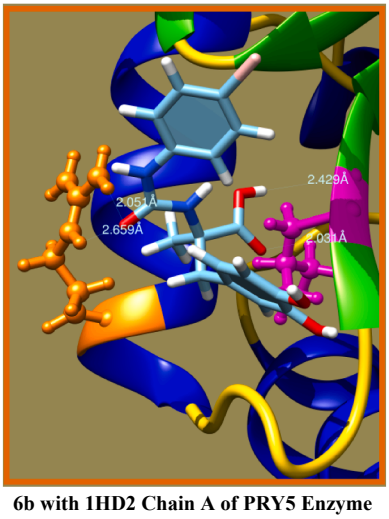

6b with 1HD2 Chain A of PRY5 Enzyme

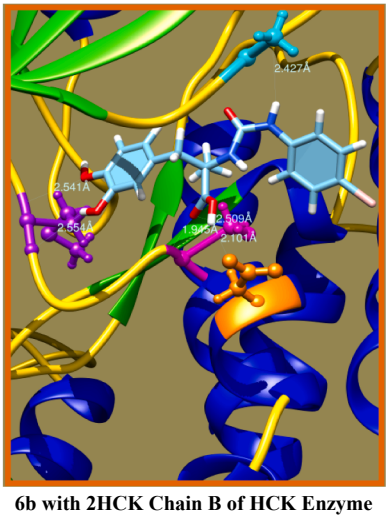

6b with 2HCK Chain B of HCK Enzyme

capillaries. IR (infrared) spectra were recorded on Bruker Alpha – EcoATR-FTIR (Attenuated Total Reflection-Fourier-Transform Infrared) interferometer having ZnSe (zinc selenide) crystal (Ettlingen, Germany) and their absorption maxima values were reported in wave numbers (ν_{max}, cm^{-1}). ^{1}H and ^{13}C NMR (Nuclear Magnetic Resonance) spectra were recorded at 400 & 100 MHz frequency respectively on Bruker 400 MHz instrument (Ettlingen, Germany) in DMSO-d_6 by using TMS (tetramethylsilane) as internal standard and their corresponding chemical shift

Table 10
Molecular Docking interactions of compound **6c** with identified enzymatic proteins.

Enzymatic Protein	Cluster Number	Cluster Rank	Binding Energy (KCal/mol)	No. of Hydrogen Bonds	H-Bond Ligand Atoms	H-Bond Receptor Atoms	Binding interaction	Bond Length (A°)	H-Bond Type
1CB4 Chain A of Superoxide Dismutase (SOD)	3	0	−7.5923	3	3	2	Ligand(CONH)——————ASP25(O)	2.573	Acceptor
							Ligand(OH)——————GLU107(O)	1.799	Acceptor
							Ligand(OH′)—————— GLU107(O)	1.828	Acceptor
1N8Q Chain A of Lipoxygenase-3 (LO)	0	0	−9.111	4	4	4	Ligand(OH)——————ASP787(O)	1.718	Acceptor
							Ligand(HO)——————ASN788(NH)	2.205	Donor
							Ligand(HN-C═O)–ASN146(NH)	2.374	Donor
							Ligand(COOH)——————VAL539(O)	1.720	Acceptor
3MNG Chain A of Peroxiredoxin-5 (PRX5)	32	4	−7.8860	3	3	3	Ligand(HNCO)————ARG86(NH)	2.203	Acceptor
							Ligand(HOCO)————LEU96(NH)	1.888	Donor
							Ligand(COOH)——————VAL94(O)	1.883	Acceptor
1OG5 Chain B of Cytochrome P450 (CP450) - 2C9	19	4	−7.8594	3	3	3	Ligand(HNCO)————PHE100(NH)	2.170	Donor
							Ligand(HOCO)————ALA103(NH)	2.383	Donor
							Ligand(OH)—————— SER365(O)	2.155	Acceptor
1DNU Chain C of Myeloperoxidase (MP)	12	7	−8.4043	2	1	2	Ligand(HOCO)——ARG239(NH)	2.186	Donor
							Ligand(HOCO)——ARG239(NH)	2.674	Donor
3NRZ Chain L of Xanthine Oxidase (XO)	3	0	−8.0734	5	4	5	Ligand(HOCO)——ARG606(NH)	2.013	Donor
							Ligand(HOCO)——ARG606(NH)	2.164	Donor
							Ligand(COOH)–GLU831(OCOH)	2.090	Acceptor
							Ligand(CONH)——————LEU607(O)	2.645	Acceptor
							Ligand(HNCO)——THR609(NH)	1.917	Donor
2CDU Chain B ofNADPH Oxidase (NO)	8	5	−7.3359	3	3	3	Ligand(OH)——————HIS396(NH)	2.079	Acceptor
							Ligand(HO)——————TYR435(OH)	2.107	Donor
							Ligand(OH′)——————PHE429(O)	2.540	Acceptor
1HD2 Chain A of Peroxiredoxin-5 (PRY5) Residue (54-214)	1	2	−7.8473	2	2	2	Ligand(HN-C═O)—ARG86(NH)	1.998	Donor
							Ligand(O═C-NH)–GLU16(OCOH)	2.556	Acceptor
2HCK Chain B of Hematopoetic Cell Kinase (HCK)	22	2	−8.1269	3	3	3	Ligand(HOCO)————SER345(OH)	2.459	Donor
							Ligand(HO)——————ASN391(NH)	2.522	Donor
							Ligand(OH′)——ASP404(COOH)	1.989	Acceptor

Table 11
Potential protein-ligand binding interactions of compound **6c** with identified enzymatic proteins.

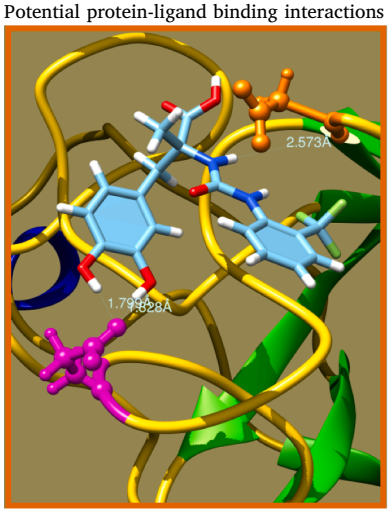

6c with 1CB4 Chain A of SOD Enzyme

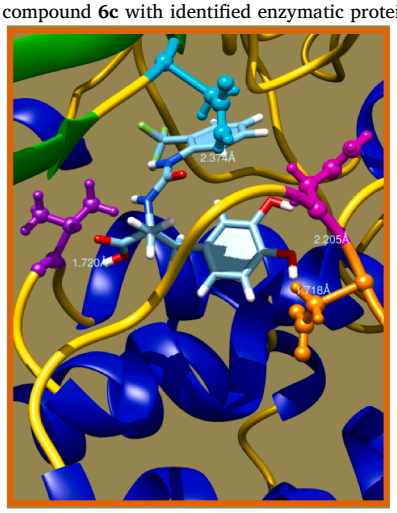

6c with 1N8Q Chain A of LO Enzyme

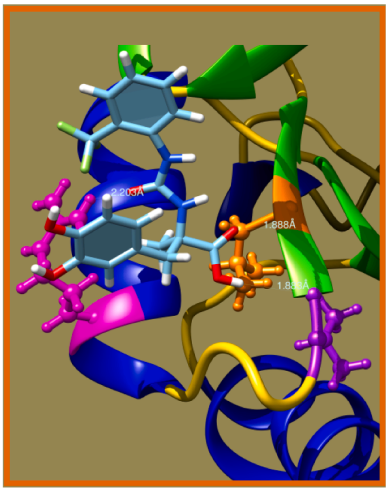

6c with 3MNG Chain A of PRXS5 Enzyme

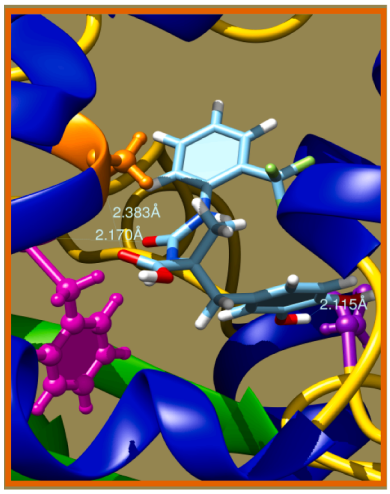

6c with 1OG5 Chain B of CP450 Enzyme

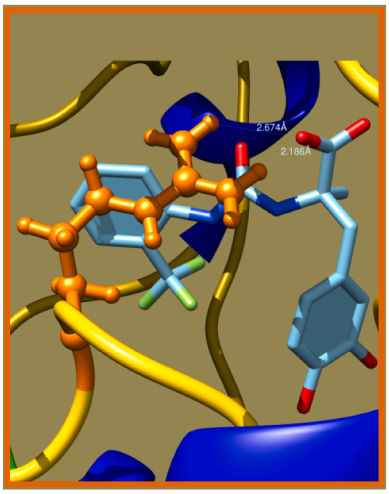

6c with 1DNU Chain C of MP Enzyme

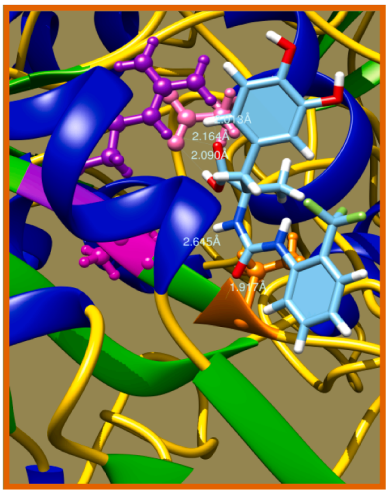

6c with 3NRZ Chain L of XO Enzyme

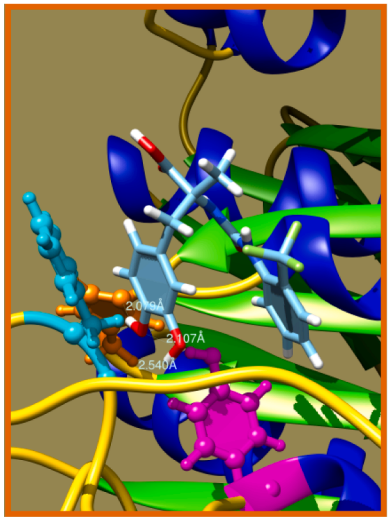

6c with 2CDU Chain B of NO Enzyme

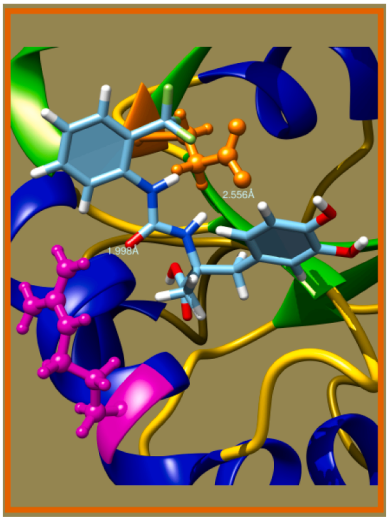

6c with 1HD2 Chain A of PRY5 Enzyme

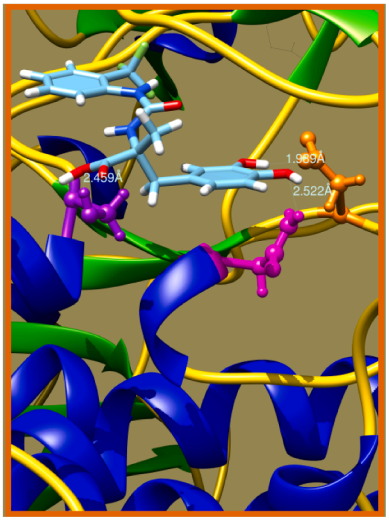

6c with 2HCK Chain B of HCK Enzyme

(δ) values were reported in ppm (parts per million). Mass spectral data presented in *m/z* ratios against corresponding percentages of abundance as recorded on Agilent LCMS instrument (Ettlingen, Germany). The elemental analysis was carried out on Thermo Finnigan Flash EA 1112 I instrument (Courtaboeuf, France). Similarly the reaction of 1-(3,4-dimethoxy phenyl)propan-2-one (**1**) and sodium cyanide in ammonium acetate/ethanol forms 2-amino-3-(3,4-dimethoxyphenyl)-2-methylpropanenitrile (**2**), then it gets hydrolyzed with 48% HBr and forms α-methyl-L-DOPA (**3**) and further used to synthesize title compounds **6a-e** (Scheme 1).

Table 12
Molecular Docking interactions of compound **6d** with identified enzymatic proteins.

Enzymatic Protein	Cluster Number	Cluster Rank	Binding Energy (KCal/mol)	No. of Hydrogen Bonds	H-Bond Ligand Atoms	H-Bond Receptor Atoms	Binding interaction	Bond Length (A°)	H-Bond Type
1CB4 Chain A of Superoxide Dismutase (SOD)	4	0	−8.4664	4	4	2	Ligand(OH)———GLU107(OCOH)	1.831	Acceptor
							Ligand(OH′)——GLU107(OCOH)	1.946	Acceptor
							Ligand(OCNH)–ASP25(OCOH)	2.232	Acceptor
							Ligand(COOH)—ASP35(OCOH)	1.839	Acceptor
1N8Q Chain Aof Lipoxygenase-3 (LO)	7	0	−8.7073	2	2	2	Ligand(OH)——ASP787(COOH)	1.927	Acceptor
							Ligand(HOCO)——TYR544(OH)	2.468	Donor
3MNG Chain A of Peroxiredoxin-5 (PRX5)	3	0	−7.8656	2	2	2	Ligand(OCNH)————VAL94(O)	2.053	Acceptor
							Ligand(COOH)————GLY82(O)	2.739	Acceptor
1OG5 Chain B of Cytochrome P450 (CP450) - 2C9	3	2	−8.3971	5	5	5	Ligand(HO)————THR364(HO)	1.982	Donor
							Ligand(OCOH)–GLN214(OCNH)	2.608	Acceptor
							Ligand(HOCO)–GLN214(HNCO)	2. 688	Donor
							Ligand(OH)———— SER365(O)	2.006	Acceptor
							Ligand(HOCO)———ASN217(NH)	2.055	Donor
1DNU Chain C of Myeloperoxidase (MP)	7	7	−8.6178	4	4	3	Ligand(OCNH′)————PHE552(O)	2.547	Donor
							Ligand(OCNH)————PHE552(O)	2.091	Donor
							Ligand(OH)————ALA389(O)	2.296	Acceptor
							Ligand(COOH)—————LEU299(O)	2.781	Acceptor
3NRZ Chain L of Xanthine Oxidase (XO)	0	3	−8.2425	4	3	4	Ligand(OH)————ASP658(NH)	2.483	Donor
							Ligand(OH)————LYS657(NH)	2.571	Donor
							Ligand(HNCO)——THR653(NH)	2.271	Donor
							Ligand(OCNH′)————ASN869(O)	2.603	Donor
2CDU Chain B ofNADPH Oxidase (NO) Protonated Histidine	12	0	−8.2147	3	3	3	Ligand(COOH)———THR112(O)	2.079	Acceptor
							Ligand(OCNH)————THR113(O)	2.107	Acceptor
							Ligand(HNCO)——ASN248(NH)	2.540	Donor
1HD2 Chain A of Peroxiredoxin-5 (PRY5) Residue (54-214)	15	0	−8.0834	3	2	3	Ligand(HO-C═O)–ARG86(NH)	2.413	Donor
							Ligand(HO-C═O)–ARG86(NH′)	2.501	Donor
							Ligand(O═C-NH′)——VAL94(O)	2.162	Acceptor
2HCK Chain B of Hematopoetic Cell Kinase (HCK)	29	0	−7.9838	5	4	5	Ligand(HO)————MET341(NH)	2.470	Donor
							Ligand(OH′)————MET341(O)	2.552	Acceptor
							Ligand(HO-C═O)–SER345(NH)	1.998	Donor
							Ligand(HO-C═O)–SER345(OH)	2.523	Donor
							Ligand(OCOH)–ASP348(OCOH)	1.989	Acceptor

Table 13
Potential protein-ligand binding interactions of compound **6d** with identified enzymatic proteins.

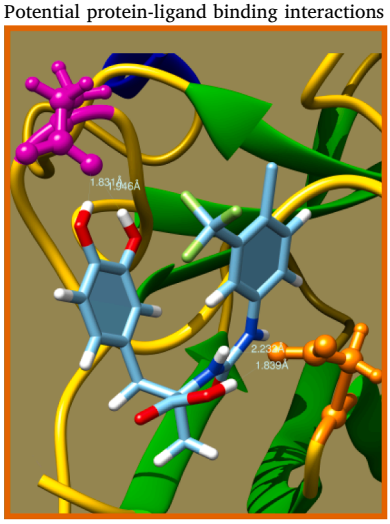

6d with 1CB4 Chain A of SOD Enzyme

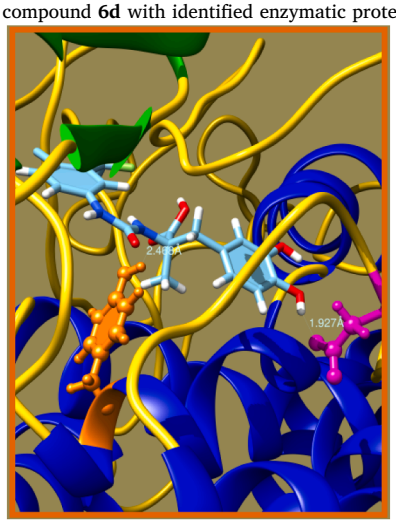

6d with 1N8Q Chain A of LO Enzyme

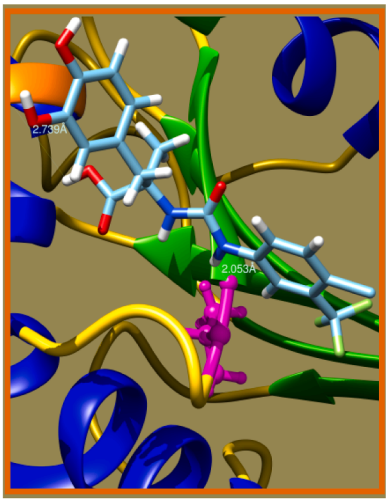

6d with 3MNG Chain A of PRXS5 Enzyme

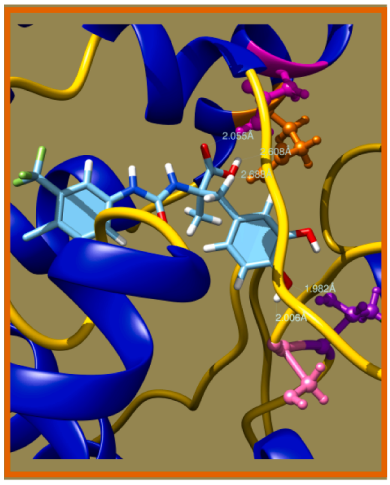

6d with 1OG5 Chain B of CP450 Enzyme

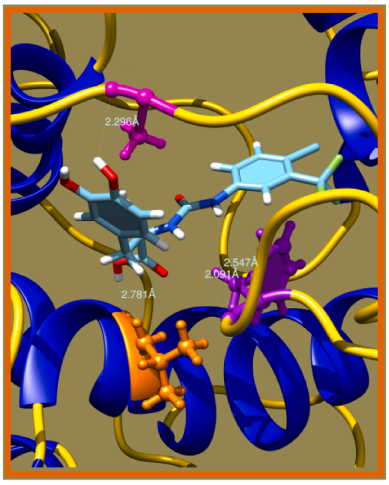

6d with 1DNU Chain C of MP Enzyme

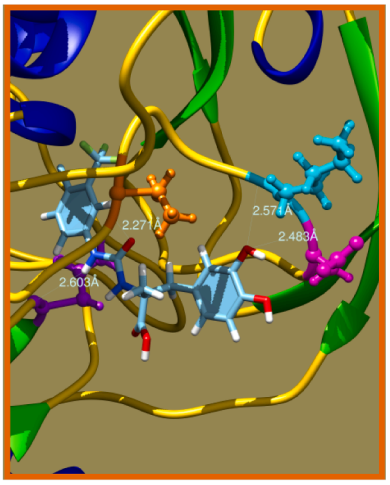

6d with 3NRZ Chain L of XO Enzyme

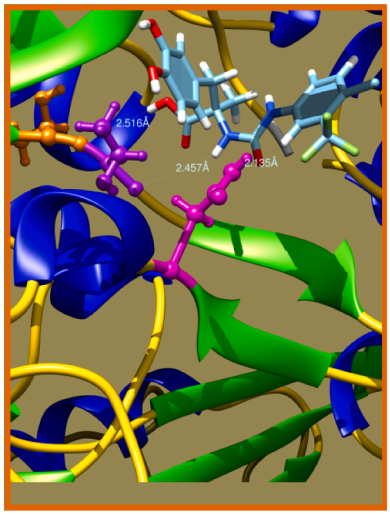

6d with 2CDU Chain B of NO Enzyme

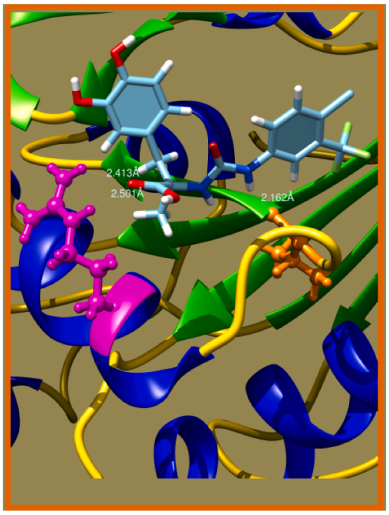

6d with 1HD2 Chain A of PRY5 Enzyme

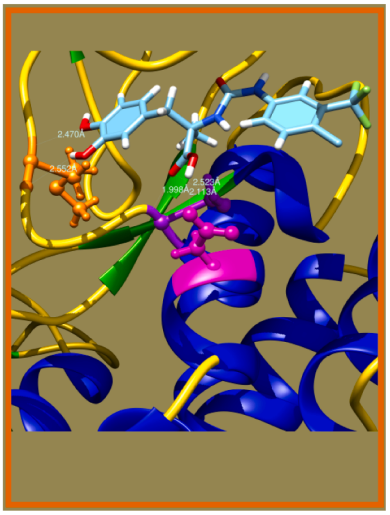

6d with 2HCK Chain B of HCK Enzyme

4.2. Antioxidant activity

Antioxidant activity of **6a-e** has been evaluated by DPPH (2,2-diphenyl-1-picrylhydrazyl), NO (nitric oxide), and H_2O_2 (hydrogen peroxide) free radical scavenging assays [59–61]. The percentage of inhibition has been evaluated from blank and test readings and referenced to ascorbic acid by using the equation.

$$\%\text{of\;inhibition} = \frac{[(A_{Control} - A_{Test})]}{(A_{Control})} \times 100$$

Table 14
Molecular Docking interactions of compound **6e** with identified enzymatic proteins.

Enzymatic Protein	Cluster Number	Cluster Rank	Binding Energy (KCal/mol)	No. of Hydrogen Bonds	H-Bond Ligand Atoms	H-Bond Receptor Atoms	Binding interaction	Bond Length (A°)	H-Bond Type
1CB4 Chain A of Superoxide Dismutase (SOD)	9	4	−7.7059	3	3	2	Ligand(OH)—GLU107(OCOH)	1.914	Acceptor
							Ligand(COOH)–ASP25(OCOH)	1.842	Acceptor
							Ligand(OCNH)–ASP25(OCOH)	2.291	Acceptor
1N8Q Chain Aof Lipoxygenase-3 (LO)	11	1	−8.8763	3	3	2	Ligand(OH)—ASP787(OCOH)	2.010	Acceptor
							Ligand(OH′)—ASP787(OCOH)	1.950	Acceptor
							Ligand(OCNH)———CYS145(O)	2.501	Acceptor
3MNG Chain A of Peroxiredoxin-5 (PRX5)	4	0	−7.7240	3	3	3	Ligand(OCNH)———VAL94(O)	2.478	Acceptor
							Ligand(OCNH′)——— VAL94(O)	2. 077	Acceptor
							Ligand(OH)———ARG86(NH)	2.178	Donor
1OG5 Chain B of Cytochrome P450 (CP450) - 2C9	33	0	−8.1349	3	3	3	Ligand(OCOH)———ASN474(O)	2.125	Acceptor
							Ligand(HOCO)—PHE476(NH)	2.130	Donor
							Ligand(OH)——— THR301(O)	2.248	Acceptor
1DNU Chain C of Myeloperoxidase (MP)	27	0	−8.1471	4	4	3	Ligand(OCNH′)———PHE552(O)	2.381	Donor
							Ligand(OCNH)———PHE552(O)	1.940	Donor
							Ligand(HO)———ALA389(NH)	2.456	Donor
							Ligand(OH′)———LEU384(O)	2.297	Acceptor
3NRZ Chain L of Xanthine Oxidase (XO)	2	1	−8.5378	3	3	3	Ligand(HO)———GLY797(NH)	2.282	Donor
							Ligand(OH)———MET1038(O)	2.569	Acceptor
							Ligand(HOCO)–SER1080(NH)	2.538	Donor
2CDU Chain B of NADPH Oxidase (NO) Protonated Histidine	8	0	−8.5546	6	6	5	Ligand(HO)———ALA11(NH)	2.187	Donor
							Ligand(′HO)———THR9(NH)	2.352	Donor
							Ligand(OH′)———THR112(O)	1.913	Acceptor
							Ligand(OCNH)———THR112(O)	1.908	Acceptor
							Ligand(OCNH′)——THR112(O)	2.163	Acceptor
							Ligand(HOCO)—ASN34(NH)	2.371	Donor
1HD2 Chain A of Peroxiredoxin-5 (PRY5) Residue (54-214)	0	1	−8.3573	5	5	4	Ligand(HO)——— VAL70(NH)	2.411	Donor
							Ligand(OH′)——— GLN68(O)	2.607	Acceptor
							Ligand(HNCO)———GLY92(NH)	2.415	Donor
							Ligand(OCNH)–GLU16(OCOH)	2.732	Acceptor
							Ligand(OCNH′)–GLU16(OCOH)	1.860	Acceptor
2HCK Chain B of Hematopoetic Cell Kinase (HCK)	6	0	−8.2492	5	5	4	Ligand(OCOH)———ALA275(O)	2.035	Donor
							Ligand(HNCO)——LYS295(NH)	2.499	Acceptor
							Ligand(HO)———SER345(OH)	2.123	Donor
							Ligand(OH)—ASP348(OCOH)	2.027	Acceptor
							Ligand(OH′)—ASP348(OCOH)	1.915	Acceptor

Table 15
Potential protein-ligand binding interactions of compound **6e** with identified enzymatic proteins.

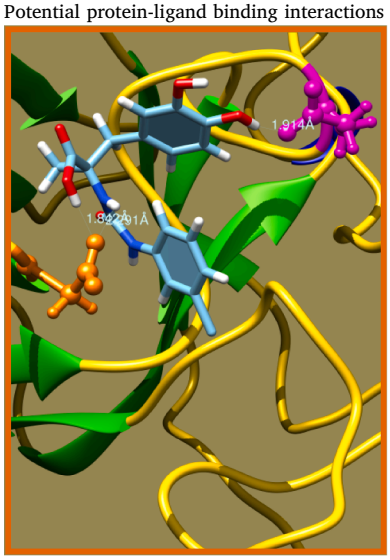

6e with 1CB4 Chain A of SOD Enzyme

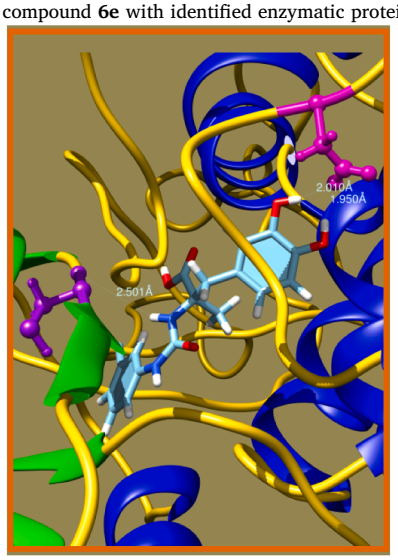

6e with 1N8Q Chain A of LO Enzyme

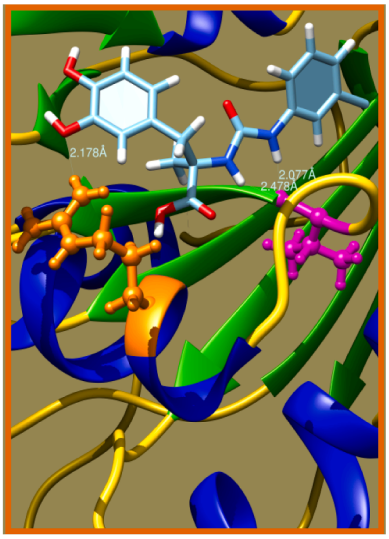

6e with 3MNG Chain A of PRXS5 Enzyme

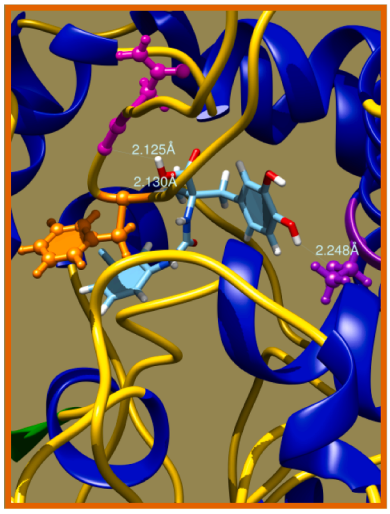

6e with 1OG5 Chain B of CP450 Enzyme

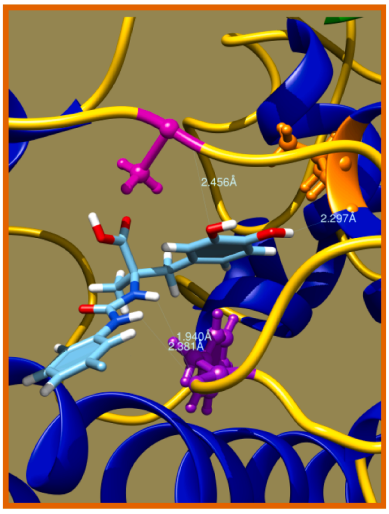

6e with 1DNU Chain C of MP Enzyme

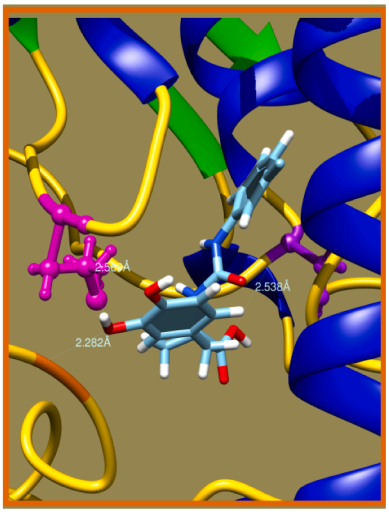

6e with 3NRZ Chain L of XO Enzyme

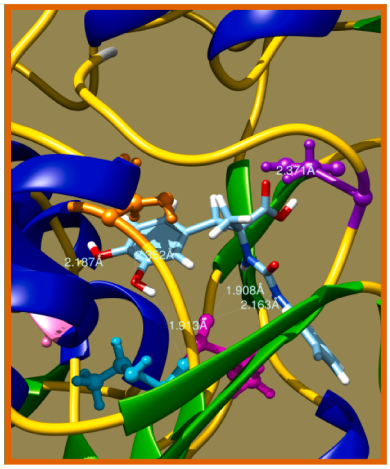

6e with 2CDU Chain B of NO Enzyme

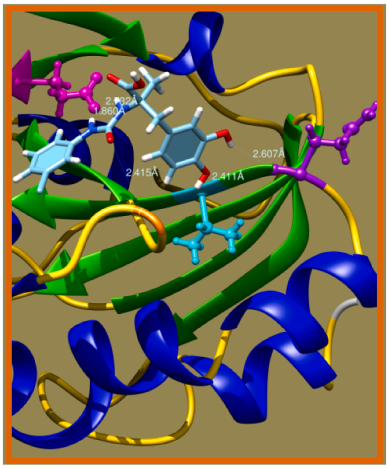

6e with 1HD2 Chain A of PRY5 Enzyme

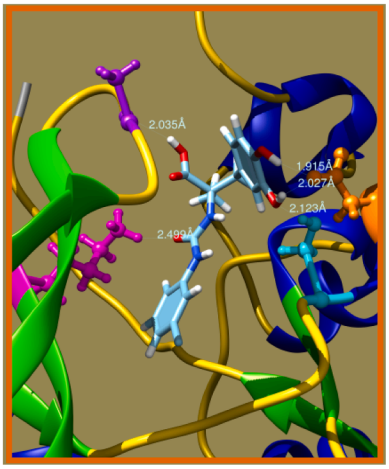

6e with 2HCK Chain B of HCK Enzyme

As such, $A_{control}$ is absorbance of ascorbic acid and A_{Test} is absorbance of **6a-e**. All tests were carried in triplicate and values were given in mean with standard deviation. The % inhibitions obtained are dose dependent against the concentrations. The IC_{50} value, the concentration necessary to decrease absorbance by 50% have been calculated by plotting the linear curves for the graphs obtained for percentage inhibitions to concentrations.

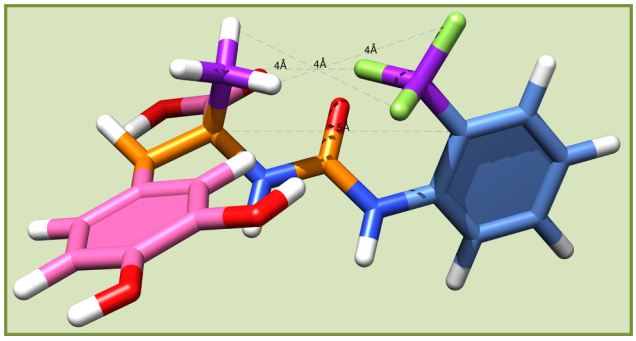

Fig. 3. Structure-activity relationship correlation of potential lead **6c.**

4.2.1. DPPH free radical scavenging assay

In this DPPH method [62], 1.0 mL of 0.1 mM concentrated methanolic DPPH solution prepared was added to 3.0 mL of methanolic test solutions of 25, 50, 75, 100 µg/mL concentrations. Then the mixture was vigorously agitated and incubated at rt for 30 min under dark conditions. The DPPH free radical scavenging activity was measured in terms of percentage of inhibition from DPPH discoloration readings by determining spectrophotometric absorbance at 517 nm. Lower absorbance of the test sample indicates it higher DPPH free radical scavenging activity [63].

4.2.2. NO free radical scavenging assay:

Theoretically, formation of nitrous acid in turns formation of azo dye has been inhibited by antioxidants and hence scavenges the free radicals indeed. According to Griess-Illosvoy method, nitric oxide generated *in situ* from nitroprusside buffer solution gets hydrolyzed aerobically and produces nitric and nitrous acids [64]. In principle, the antioxidants inhibit the nitrous acid free radical generation from sodium nitroprusside and hence we estimate the nitrous acid that is liberated and which reacts with Griess reagent and produces a purple azo dye. Practically, 3 mL of composite analyte mixture (0.5 mL of analyte + 2 mL of 10 mM sodium nitroprusside + 0.5 mL saline phosphate buffer) with 25, 50, 75, 100 µg/mL concentrations were prepared and incubated for 2.5 h at 25 °C. Then, 0.5 mL of mixture was treated with 1.5 mL Griess reagent [1.0% sulphanilamide + 0.1% N-(1-naphtyl) ethylene diamine dihydrochloride + 2.5% H_3PO_4] and then the chromophoric absorbance of formed azo dye was measured at 540 nm on UV–visible spectrophotometer. Greater the absorbance of analyte entitles higher NO scavenging activity [65].

4.2.3. H_2O_2 free radical scavenging assay

In this method, ability of an analyte to effectively scavenge the hydrogen peroxide free radical has been determined [66]. The analytic solution was prepared by the adding 2 mL of hydrogen peroxide to test solutions of 25, 50, 75, 100 µg/mL concentrations in phosphate buffer saline of p^H 7.4. The absorbance of hydrogen peroxide was measured at 230 nm against blank (phosphate buffer without hydrogen peroxide) solution After 10 min. The increased absorbance of test compounds shows enhanced reducing power [67].

5. Experimental

5.1. Chemistry

(*α*-methyl-*L*-Dopa (**3**), 1 mmol, 211 mg) and triethyl amine (TEA, **5**, 0.6 mL, 1 mmol) base were taken in 5 mL of THF in to a round bottom flask, thoroughly stirred to get uniform solution. To this a solution of 2-fluoro phenyl isocyanate (**4a**, 1 mmol, 137 mg) in 5 mL of THF is added slowly and stirred for a period of 3 h at 40–50 °C [68]. After completion of reaction, as indicated by TLC, the reaction mixture was concentrated under vacuum distillation to get 3-(3,4-dihydroxyphenyl)-2-(3-(2-fluorophenyl)ureido)-2-methylpropanoic acid **(6a)**, purified by column chromatography by using ethyl acetate: hexane (1:4) as an eluent and obtained the pure product. Similarly **6b-e** also have been synthesized by same procedure and characterized by IR, ^{1}H & ^{13}C NMR & MASS spectral and elemental analytical studies. Spectral and elemental analysis data of compounds **6a-e** has been provided as follows.

5.1.1. 3-(3,4-dihydroxyphenyl)-2-(3-(2-fluorophenyl)ureido)-2-methylpropanoic acid *(6a)*

White solid; Yield 90%; mp: 175–178 °C; IR (cm^{-1}, ν_{max}): 3423(NH), 3287(OH), 1646 (C═O), 808 (C-F); ^{1}H NMR (400 MHz, DMSO-d_6): δ 10.98 (s, 1H, −COOH), 8.15 (s, 2H, NH), 7.22–6.98 (m, 4H, Ar-H), 6.60 (s, 1H, Ar-H), 6.53(d, 1H, J = 12, Ar-CH), 6.47 (d, 1H, J = 8, Ar-CH), 5.55(s, 1H, OH), 5.31(s, 1H, OH), 3.32 (s, 1H, CH), 2.46 (s, 1H, CH), 1.61 (s, 3H, CH_3) ppm; ^{13}C NMR (100 MHz, DMSO-d_6): δ 170.0, 153.7, 152.5, 151.3, 143.1, 139.9, 127.8, 125.0, 123.2, 121,1, 118.2, 115.4, 113.8, 70.1, 40.0, 27.1; ESI-MS *m/z (%)*: 349 $[M+H]^{+\cdot}$; Anal. Calcd for $C_{17}H_{17}FN_2O_5$ (%): C 58.62; H 5.92; N 8.04; Found: C 58.72; H 4.23; N 8.12.

5.1.2. (3-(4-bromophenyl)ureido)-3-(3,4-dihydroxyphenyl)-2-methylpropanoic acid *(6b)*

White solid; Yield: 90%; mp: 181–183 °C; IR (cm^{-1}, ν_{max}): 3420(NH), 3295(OH), 1657(C═O), 666 (C-Br); ^{1}H NMR (400 MHz, DMSO-d_6): δ 11.21 (s, 1H, −COOH), 9.65(s, 2H, NH), 7.55–6.98 (m, 4H, Ar-H), 6.65 (s, 1H, Ar-H), 6.65(d, 1H, J = 8, Ar-CH), 6.54 (d, 1H, J = 8, Ar-CH), 5.71(s, 1H, OH), 5.52(s, 1H, OH), 3.42 (s, 1H, CH), 2.56 (s, 1H, CH), 1.71 (s, 3H, CH_3) ppm; ^{13}C NMR (100 MHz, DMSO-d_6): 172.0,

Table 16
ADMET properties predicted for compounds **6a-e.**

Compounds	*in vivo* blood-brain barrier penetration (C.brain/C.blood)[a]	*in vitro* Caco-2 cell permeability (nm/sec)[b]	*in vitro* plasma protein binding (%)[c]	*in vitro* MDCK cell permeability (nm/sec)[d]	Human intestinal absorption (HIA, %)[e]	Toxicity[f]
6a	0.294438	21.0311	82.476035	2.08243	77.637382	Negative
6b	0.501142	20.3174	86.182762	0.031757	86.697345	Negative
6c	0.421278	19.8243	92.817459	0.152409	79.500743	Negative
6d	0.749112	19.8126	86.045284	0.0564461	85.137192	Negative
6e	0.497189	18.8199	83.274615	2.42001	84.170512	Negative
3	0.472612	21.1075	9.079006	14.7944	61.912798	Negative
Ascorbic Acid	0.172436	2.65695	2.790093	0.72561	29.075921	Negative

[a] Blood-Brain Barrier (BBB) penetration = [Brain]/[Blood].
[b] Caco-2 cells are derived from human colon adenocarcinoma, possess multiple drug transport pathways through intestinal epithelium.
[c] % of drug binds to plasma protein.
[d] MDCK cell system used as tool for rapid permeability screening.
[e] Human intestinal absorption is the sum of bioavailability and absorption evaluated from ratio of excretion or cumulative excretion in urine, bile and feces.
[f] *in vitro* Ames test by Metabolic & Non-metabolic activated TA100 & TA1535 strains collected from rat liver homogenate.

Table 17
QSAR Properties of the compounds **6a-e.**

Entry	Lipinski Parameters						Veber Parameters			Other Parameters			
	MW	HB Don	HB Acc	logP (o/w)	MR	Lip Vio	TPSA	No. of RB	Veb Vio	No. of H	V. Volume	ρ	Solubility
6a	348.33	5	6	1.81	87.79	0	118.88	5	0	17	237.2	1.467	−3.26
6b	409.24	5	6	2.44	95.48	0	118.88	5	0	17	249.2	1.641	−3.78
6c	398.34	5	6	2.56	92.77	0	118.88	6	0	18	266.5	1.494	−3.72
6d	432.78	5	6	3.17	97.67	0	118.88	6	0	18	278.5	1.553	−4.46
6e	364.79	5	6	2.32	92.69	0	118.88	5	0	17	245.0	1.488	−3.68
3	211.22	5	5	−1.86	53.89	0	103.78	3	0	10	150.4	1.403	−1.06
Ascorbic Acid	178.14	6	4	−2.89	35.66	0	107.22	2	0	6	100.8	1.766	0.08

MW: Molecular weight; HB Don: Hydrogen bond donors; HB Acc: Hydrogen bond acceptors; logP: octanol to water partition coefficient; MR: Molecular refractivity (cm^3/mol); Lip Vio: Lipinski Violations; TPSA: Total polar surface area; No. of RB: Number of rotatable bonds; Veb Vio: Veber Violations; No. of 'H': Number of Hydrophobic Atoms; V. Volume: *Van der Waals* volume; ρ: Density (gm/cc).

Table 18
Bioactivity and toxicity risks of compounds **6a-e.**

Compounds	Structure	Bioactivity						Toxicity Risks	
		GPCRL	ICM	KI	NRL	PI	EI	Drug-likeness	Drug Score
6a	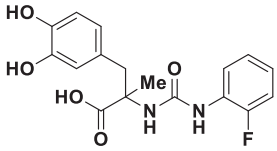	0.27	0.04	−0.00	−0.07	0.31	0.09	−0.91	0.54
6b	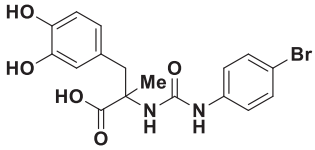	0.22	−0.03	−0.08	−0.16	0.19	0.03	−1.42	0.27
6c	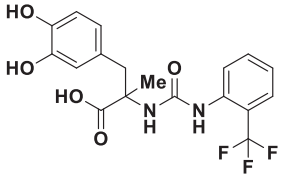	0.29	0.10	−0.04	0.09	0.27	0.09	−8.78	0.38
6d	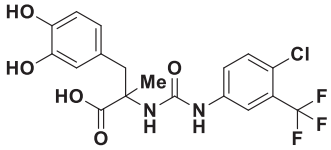	0.28	0.08	0.01	0.07	0.20	0.03	−7.45	0.32
6e	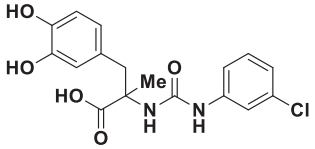	0.31	0.04	−0.05	−0.08	0.23	0.05	0.48	0.64
3	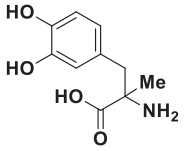	0.06	0.08	−0.53	−0.48	0.13	0.07	−1.88	0.44
Ascorbic Acid	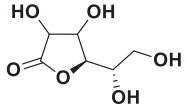	−0.51	−0.45	−1.29	−1.20	−0.87	−0.04	−6.5	0.49

GPCRL: G protein-coupled receptor Ligand; ICM: Ion channel modulator; KI: Kinase inhibitor; NRL: Nuclear receptor ligand; PI: Protease inhibitor; EI: Enzyme inhibitor.

154.1, 153.1, 151.7, 143.5, 140.9, 128.2, 125.5, 122.9, 122.0, 119.1, 115.8, 114.2, 71.2, 41.1, 26.9 ppm; ESI-MS *m/z (%)*: 410 $[M+H]^{+\cdot}$; Anal. Calcd for $C_{17}H_{17}BrN_2O_5$: C 50.12, H 4.28, N 6.90; Found: C 49.89, H 4.19, N 6.85.

5.1.3. 3-(3,4-dihydroxyphenyl)-2-methyl-2-(3-(2-(trifluoromethyl)phenyl) ureido)propanoic acid ***(6c)***

White solid; Yield 90%; mp: 191–193 °C; IR (cm^{-1}, ν_{max}): 3442(NH), 3321(OH), 1666 (C═O), 809 (C-F); ^{1}H NMR (400 MHz,

DMSO-d_6): δ 10.95 (s, 1H, −COOH), 9.09(s, 2H, NH), 7.25–7.11 (m, 3H, Ar-H), 6.86 (s, 1H, Ar-H), 6.66 (s, 1H, Ar-H), 6.65(d, 1H, J = 8, Ar-CH), 6.55 (d, 1H, J = 8, Ar-CH), 5.61(s,1H, OH), 5.42(s, 1H, OH), 3.35 (s, 1H, CH), 2.46 (s, 1H, CH), 1.65 (s, 3H, CH_3) ppm; ^{13}C NMR (100 MHz, DMSO-d_6): δ 169.0, 154.5, 152.9, 151.9, 143.6, 140.5, 128.1, 125.2, 123.9, 121.6, 118.5, 115.7, 113.5, 70.5, 40.2, 27.3 ppm; ESI-MS *m/z (%)*: 397 $[M-H]^{+\cdot}$; Anal. Calcd for $C_{18}H_{17}F_3N_2O_5$: C 54.57, H 4.30, N 7.14; Found: C 54.52, H 4.12, N 7.03.

5.1.4. 2-(3-(4-chloro-3-(trifluoromethyl)phenyl)ureido)-3-(3,4-dihydroxyphenyl)-2-methylpropanoic acid **(6d)**

White solid; Yield 90%; mp: 195–198 °C; IR (cm^{-1}, ν_{max}): 3401(NH), 3295(OH), 1651(C═O), 825(C-F), 762(C-Cl); ^{1}H NMR (400 MHz, DMSO-d_6): δ 10.92 (s, 1H, −COOH), 9.05 (2H, −NH),), 8.15(s,1H, Ar-H), 8.15 (d, 1H J = 12, Ar-H), 8.25(d, 1H, J = 16, Ar-H), 6.92(d, 1H, J = *12*, Ar-H)7.21 (d, 1H, J = *8*, Ar-H), 6.62 (s, 1H, Ar-H), 5.51(s,1H, OH), 5.42(s, 1H, OH), 3.42 (s, 1H, CH), 2.35 (s, 1H, CH), 1.85 (s, 3H, CH_3) ppm; ^{13}C NMR (100 MHz, DMSO-d_6): δ 172.0, 155.1, 154.2, 152.1, 143.3, 141.2, 128.5, 125.5, 124.7, 122.9, 119.1, 115.9, 114.5, 70.3, 40.6, 27.5 ppm; ESI-MS *m/z (%)*: 433 $[M+H]^{+\cdot}$; Anal. Calcd for $C_{18}H_{16}ClF_3N_2O_5$: C 49.95, H 3.73, N 6.52; Found: C 50.21, H 3.55, N 6.47.

5.1.5. 2-(3-(3-chlorophenyl)ureido)-3-(3,4-dihydroxyphenyl)-2-methylpropanoic acid **(6e)**

White solid; Yield 90%; mp: 178–180 °C; IR (cm^{-1}, ν_{max}): 3429 (NH), 3285 (OH), 1642(C═O), 755 (C-Cl); ^{1}H NMR (400 MHz, DMSO-d_6): δ 11.25 (s, 1H, −COOH), 9.12 (2H, −NH), 8.25 (s, 1H, Ar-H), 7.62 (s, 1H, Ar-H), 6.56(d, 1H, J = 8, Ar-H), 6.95 (d, 1H, J = 12, Ar-H), 7.51(d, 1H, J = 8, Ar-H), 7.62 (d, 1H, J = 12, Ar-H), 7.42 (d, 1H, J = 8, Ar-H), 5.53(s,1H, OH), 5.32(s, 1H, OH), 3.39 (s, 1H, CH), 2.48 (s, 1H, CH), 1.65 (s, 3H, CH) ppm; ^{13}C NMR (100 MHz, DMSO-d_6): δ 172.0, 154.7, 153.5, 152.3, 144.1, 140.9, 128.8, 126.0, 124.2, 121.9, 119.6, 115.5, 114.2, 70.5, 41.5, 27.6 ppm; ESI-MS *m/z (%)*: 365 $[M+H]^{+\cdot}$; Anal. Calcd for $C_{17}H_{17}ClN_2O_5$: C 56.97, H 4.70, N 7.78; Found: C 56.22, H 4.65, N 7.72.

5.2. Antioxidant activity

The newly synthesized urea derivatives **(6a-e)** of α-Methyl-L-DOPA were evaluated for DPPH free radical, NO free radical and H_2O_2 free radical scavenging assays at concentrations of 25, 50, 75 and 100 μg/mL and referenced to ascorbic acid standards. Then calculated their IC_{50} (half maximal concentration) values. The analysis of results revealed that urea derivatives **6c** and **6d** were exhibited potential antioxidant activity.

5.3. Molecular docking studies

The mechanistic inhibition of proliferation of ROS *in vivo* by **6a-e** has been assessed by molecular docking interactions studies. During so, the crystal structures of proteins were obtained as PDB files from protein data bank and used after removal of bound ligands, water and cofactors from the environment. The .pdb files and .mol2 files of **6a-e** were generated from Chem3D Pro 14.0 of ChemBioOffice software and docked with all proteins on Swiss Dock [69]. For the better understanding of anti-oxidant potentiality, study has been extended to the substrate α-methyl-L-DOPA **(3)** and standard ascorbic acid. The interactive structures were identified in energy minimized optimizations with 0.100 of minimum root mean standard deviation gradient and the binding modes are visualized by UCSF Chimera [70]. The binding energies of best fit interactions of substrate ligands with target receptors in 1CB4 protein (chain A) of superoxide dismutase (SOD) enzyme, 1N8Q protein (chain A) of Lipoxygenase-3 (LO) enzyme, 3MNG protein (chain A) of Peroxiredoxin-5 (PRXS5) enzyme, 1OG5 protein (chain B) of Cytochrome p450 (CP450) enzyme, 1DNU protein (chain C) of Myeloperoxidase (MP) enzyme, 3NRZ protein (chain L) of Xanthine dehydrogenase/oxidase (XO) enzyme, 2CDU protein (Chain B) of NADPH oxidase (NO) enzyme, 1HD2 Protein (Chain A) of Peroxiredoxin 5 (PRY5) enzyme and 2HCK protein (Chain B) of Hematopoetic cell kinase (HCK) enzyme were identified in macromolecular structural environment and identified that **6a-e** are effectively binding with all the proteins identified and presented in Table 6–15.

5.4. ADMET properties

ADMET properties of **6a-e** have envisioned on preADMET online server [71], which helped to realize their potentialities with regard to *in vivo* BBB (blood brain barrier) penetration, *in vitro* PPB (plasma protein binding), *in vitro* Caco-2 cell permeability, %HIA (human intestinal absorption) and *in vitro* MDCK (Maden Darby Canine Kidney) cell permeability properties. In continuation, the toxicity properties *viz.*, mutagenic, tumarogenic, irritant and reproductive effects also helped to ensure the drug-likeness. The BBB is fulfilled with intensely bound endothelial cells which restrict the ability of a compound that is to be carried into the bloodstream by passing through the administered route. The study of BBB penetration rate (BBB = [Brain]/[Blood]) assists us to examine the capability of a compound to percolate through blood-brain barrier, which is a *vital* in ascribing central nervous system (CNS) activity to the archives of pharmaceutical properties of a compound. The compounds which are capable to pass through the BBB are designated as CNS active (BBB penetration rate > 0.40) and which are inept are called CNS-inactive (BBB penetration rate < 0.40) compounds. On the other hand Caco-2 (human colon adenocarcinoma based cells) cells inter relates with intestinal epithelium system in multiple drug transport pathways like transcellular, paracellular and active efflux transports. The compounds conquering *in vitro* Caco-2 cell permeability value < 4 are poor permeable, compounds in midst of 4–70 are moderately permeable and compounds with value > 70 are extremely permeable and are easily transported to cellular biochemical processes. Besides, the degree of PPB impacts the level of distribution of unbound compound in body tissues and the amount of unbound compound which is distributed over the cellular sites of action, will further metabolizes and excreted from the system. The percentage of PPB (*in vitro*) categorizes the compounds as strongly bound if %PPB > 90% and as weakly bound if %PPB < 90% and this degree of PPB of a compound determines its action as well as efficiency. Furthermore the MDCK cell system is identified as a useful tool to screen out the rapid permeability of a compound and to decide its potentiality as its cellular life span is smaller than the life span of Caco-2 cells and therefore the correlation will be so high. Mainly, *in vitro* MDCK permeability value < 25 designates the compounds as poor permeable, value in between the range of 25–500 designates the compounds are reasonably permeable and value > 500 designates the compounds are greatly permeable. Similarly the % HIA is considered as the percentage of a compound that is getting orally administered in to the hepatic portal vein. Mostly, it is expressed as comprehensive bioavailability and absorption which are measured from the ratio of aggregate excretion in bile, urine and feces. The % HIA in the range of 0–20 designates poor absorbance, 20–70 designates moderate absorbance and 70–100 designates good absorbance of a compound. In toxicology perception, it is significant to concern about the toxicology aspects of a compound as in to exclude the toxicity risks in its design. The negative toxicology result sustain the molecules under study as safer drugs as they are prone to mutagenicity, carcinogenicity and human ether-a-go-go related gene (HERG) channel inhibition on its administration *in vivo* (Table 16).

5.5. QSAR studies

The QSAR descriptors of **6a-e** have been evaluated from molinspiration online server [72] specifically, molinspiration engine v2018.10 is used for property exploration and molinspiration engine

v2018.03 is used for bioactivity score exploration. Similarly, drug properties were predicted from OSIRIS online property explorer [73] and the consolidated descriptors were given under the heads of Lipinski & Veber Parameters and were presented in in Table 17. These predictions are very much helpful in interpreting the physico-chemical interactions of title compounds with their targets and ultimately assisted in ascertaining their drug properties by correlating with the bioactivity & toxicity risks studies.

5.6. Bioactivity and toxicity risk studies

The bioactivity & toxicity risks like GPCR (G protein-coupled receptor) ligand property, ICM (ion channel modulator), KI (kinase inhibitor) and NRL (nuclear receptor ligand) interactions, PI (protease inhibitor) and EI (enzyme inhibitor) inhibitions, drug-likeness and drug scores of **6a-e** have assessed **(**Table 18**)** and proved title compounds as potential non-toxic molecules.

Declaration of Competing Interest

The authors declare that they have no known competing financial interests or personal relationships that could have appeared to influence the work reported in this paper.

Acknowledgments

The authors Dr. Avula Vijaya Kumar Reddy and Prof. Dr. Grigory V. Zyryanov are thankful to Ural Federal University for support and also acknowledge the financial support of the Russian Science Foundation, Moscow, Russian Federation (RSF Grant No.: 18-13-00365).

Appendix A. Supplementary material

Supplementary data to this article can be found online at https://doi.org/10.1016/j.bioorg.2020.103708.

References

[1] G. Perry, A. Nunomura, K. Hirai, X. Zhu, M. Prez, J. Avila, R.J. Castellani, C.S. Atwood, G. Aliev, L.M. Sayre, A. Takeda, M.A. Smith, Is oxidative damage the fundamental pathogenic mechanism of Alzheimer's and other neurodegenerative diseases? Free Radic. Biol. Med. 33 (2002) 1475–1479, https://doi.org/10.1016/S0891-5849(02)01113-9.

[2] H. Zheng, S. Gal, L.M. Weiner, O. Bar-Am, A. Warshawsky, M. Fridkin, M.B.H. Youdim, Novel multifunctional neuroprotective iron chelator-monoamine oxidase inhibitor drugs for neurodegenerative diseases: *in vitro* studies on antioxidant activity, prevention of lipid peroxide formation and monoamine oxidase inhibition, J. Neurochem. 95 (2005) 68–78, https://doi.org/10.1111/j.1471-4159.2005.03340.x.

[3] L.P. Köse, İ. Gülçin, A.C. Gören, J. Namiesnik, A.L.M. Ayala, S. Gorinstein, LC-MS/MS analysis, antioxidant and anticholinergic properties of *galanga (Alpinia officinarum Hance) rhizomes*, Ind. Crop. Prod. 74 (2015) 712–721, https://doi.org/10.1016/j.indcrop.2015.05.034.

[4] E. Bursal, İ. Gülçin, Polyphenol contents and *in vitro* antioxidant activities of lyophilized aqueous extract of *kiwifruit (Actinidia deliciosa)*, Food Res. Int. 44 (2011) 1482–1489, https://doi.org/10.1016/j.foodres.2011.03.031.

[5] V. Matteo, E. Esposito, Biochemical and therapeutic effects of antioxidants in the treatment of Alzheimer's disease, Parkinson's disease, and Amyotrophic Lateral Sclerosis, CNS Neurol. Disord.-DR 2 (2003) 95–107, https://doi.org/10.2174/1568007033482959.

[6] İ. Gülçin, E. Bursal, M.H. Şehitoğlu, M. Bilsel, A.C. Gören, Polyphenol contents and antioxidant activity of lyophilized aqueous extract of *propolis* from *Erzurum*, Turkey, Food Chem. Toxicol. 48 (2010) 2227–2238, https://doi.org/10.1016/j.fct.2010.05.053.

[7] Y.G. Sherki, E. Melamed, D. Offen, Oxidative stress induced-neurodegenerative diseases: the need for antioxidants that penetrate the blood brain barrier, Neuropharmacology 40 (2001) 959–975, https://doi.org/10.1016/S0028-3908(01)00019-3.

[8] S. Ni, Y. Yuan, J. Huang, X. Mao, M. Lv, J. Zhu, X. Shen, J. Pei, L. Lai, H. Jiang, J. Li, Discovering potent small molecule inhibitors of Cyclophilin A using de Novo drug design approach, J. Med. Chem. 52 (2009) 5295–5298, https://doi.org/10.1021/jm9008295.

[9] T.M. Dawson, J.P. Steiner, W.E. Lyons, M. Fotuhi, M. Blue, S.H. Snyder, The immunophilins, FK506 binding protein and cyclophilin, are discretely localized in the brain: relationship to calcineurin, Neuroscience 62 (1994) 569–580, https://doi.org/10.1016/0306-4522(94)90389-1.

[10] F. Azam, I.A. Alkskas, M.A. Ahmed, Synthesis of some urea and thiourea derivatives of 3-phenyl/ethyl-2-thioxo-2,3-dihydrothiazolo[4,5-*d*]pyrimidine and their antagonistic effects on haloperidol-induced catalepsy and oxidative stress in mice, Eur. J. Med. Chem. 44 (2009) 3889–3897, https://doi.org/10.1016/j.ejmech.2009.04.007.

[11] S. Nikam, Urea and thiourea derivatives of substituted quinoxaline 2,3-diones as glutamate receptor antagonists, WO1998023599, 1998. https://patentscope.wipo.int/search/en/detail.jsf?docId=WO1998023599&tab=PCTDOCUMENTS&_cid=P22-K4V5NP-53993-1.

[12] M. Mahdavi, M.S. Shirazi, R. Taherkhani, M. Saeedi, E. Alipour, F.H. Moghadam, A. Moradi, H. Nadri, S. Emami, L. Firoozpour, A. Shafiee, A. Foroumadi, Synthesis, biological evaluation and docking study of 3-aroyl-1-(4-sulfamoylphenyl)thiourea derivatives as 15-lipoxygenase inhibitors, Eur. J. Med. Chem. 82 (2014) 308–313, https://doi.org/10.1016/j.ejmech.2014.05.054.

[13] M.M. Choi, E.A. Kima, H.G. Hahn, K.D. Nam, S.J. Yang, S.Y. Choi, T.U. Kim, S.W. Cho, J.W. Huh, Protective effect of benzothiazole derivative KHG21834 on amyloid β-induced neurotoxicity in PC12 cells and cortical and mesencephalic neurons, Toxicology 239 (2007) 156–166, https://doi.org/10.1016/j.tox.2007.07.010.

[14] O.W. Kwon, E. Moon, M.A. Chari, T.W. Kim, A.J. Kim, P. Lee, K.H. Ahn, S.Y. Kim, A substituted 3,4-dihydropyrimidinone derivative (compound D22) prevents inflammation mediated neurotoxicity; role in microglial activation in BV-2 cells, Bioorg. Med. Chem. Lett. 22 (2012) 5199–5203, https://doi.org/10.1016/j.bmcl.2012.06.082.

[15] M.R. Mannam, S.R. Devineni, C.M. Pavuluri, N.R. Chamarthi, R.S.P. Kottapalli, Urea and thiourea derivatives of 3-(trifluoromethyl)-5,6,7,8-tetrahydro-[1, 2, 4] triazolo[4,3-a]pyrazine: Synthesis, characterization, antimicrobial activity and docking studies, Phosphorus, Sulfur Silicon Relat. Elem. 194 (2019) 922–932, https://doi.org/10.1080/10426507.2019.1577845.

[16] M.R. Mannam, S. Srimurugan, P. Kumar, N.R. Chamarthi, K.R.S. Prasad, Synthesis of novel 3-[(2R*)-2-[(2S*)-6-fluoro-3,4-dihydro-2*H*-chromen-2-yl]-2-hydroxyethyl]-urea/thiourea derivatives and evaluation of their antimicrobial activities, Phosphorus, Sulfur Silicon Relat. Elem. 195 (2020) 65–74, https://doi.org/10.1080/10426507.2019.1635596.

[17] D.R. Shah, R.P. Modh, D.V. Desai, K.H. Chikhalia, Novel urea/thiourea derivatives of quinazolin-4(3*H*)-one: design, synthesis, antimicrobial and anti-TB study, Lett. Drug Des. Disco. 11 (2014) 560–571, https://doi.org/10.2174/1570180810666131122003517.

[18] P. Vedavathi, H. Sudhamani, C.N. Raju, Synthesis and antimicrobial activity of new urea and thiourea derivatives of (2′-(1*H*-tetrazol-5-yl)biphenyl-4-yl)methanamine, Res. Chem. Int. 43 (2017) 3251–3263, https://doi.org/10.1007/s11164-016-2823-1.

[19] H.M. Faidallah, K.A. Khan, A.M. Asiri, Synthesis and biological evaluation of new 3-trifluoromethylpyrazolesulfonyl-urea and thiourea derivatives as antidiabetic and antimicrobial agents, J. Fluor. Chem. 132 (2011) 131–137, https://doi.org/10.1016/j.jfluchem.2010.12.009.

[20] S.R. Devineni, M. Golla, N.R. Chamarthi, B. Meriga, M.S. Saddala, U.R. Asupathri, 2-Amino-2,3-dihydro-1*H*-2λ^5-[1,3,2]diazaphospholo [4,5-*b*]pyridin-2-one-based urea and thiourea derivatives: synthesis, molecular docking study and evaluation of anti-inflammatory and antimicrobial activities, Med. Chem. Res. 25 (2016) 751–768, https://doi.org/10.1007/s00044-016-1518-x.

[21] H. Sudhamani, S.K.T. Basha, S. Adam, S. Madhusudhana, A.U. Rani, C.N. Raju, Synthesis and evaluation of urea and thiourea derivatives of lopinavir intermediate as potent antimicrobial, antioxidant agents and molecular docking studies against Staphopain, Res. Chem. Int. 43 (2017) 103–120, https://doi.org/10.1007/s11164-016-2609-5.

[22] H. Sudhamani, S.K.T. Basha, S. Adam, B.V. Bhaskar, C.N. Raju, Synthesis, characterization, and bio-activity evaluation of thiourea derivatives of epinephrine as antimicrobial and antioxidant agents: molecular docking studies, Monatsh. Chem. 148 (2017) 1525–1537, https://doi.org/10.1007/s00706-017-1938-4.

[23] M. Chandrasekhar, G.S. Prasad, C. Venkataramaiah, C.N. Raju, K. Seshaiah, W. Rajendra, Synthesis, spectral characterization, docking studies and biological activity of urea, thiourea, sulfonamide and carbamate derivatives of imatinib intermediate, Mol. Divers. 23 (2019) 723–738, https://doi.org/10.1007/s1103.

[24] M.K. Prashanth, H.D. Revanasiddappa, Synthesis and antioxidant activity of novel quinazolinones functionalized with urea/thiourea/thiazole derivatives as 5-lipoxygenase inhibitors, Lett. Drug Des. Discov. 11 (2014) 712–720, https://doi.org/10.2174/1570180811666131230235157.

[25] C.S. Shantharam, D.M.S. Vardhan, R. Suhas, M.B. Sridhara, D.C. Gowda, Inhibition of protein glycation by urea and thiourea derivatives of glycine/proline conjugated benzisoxazole analogue - Synthesis and structure-activity studies, Eur. J. Med. Chem. 60 (2013) 325–332, https://doi.org/10.1016/j.ejmech.2012.12.029.

[26] J.R. Brown, E.J. North, J.G. Hurdle, C. Morisseau, J.S. Scarborough, D. Sun, J. Korduláková, M.S. Scherman, V. Jones, A. Grzegorzewicz, R.M. Crew, M. Jackson, M.R.M. Neil, R.E. Lee, The structure-activity relationship of urea derivatives as anti-tuberculosis agents, Bioorg. Med. Chem. 19 (2011) 5585–5595, https://doi.org/10.1016/j.bmc.2011.07.034.

[27] M. Díaz, H.D. Lucio, E. Moreno, S. Espuelas, C. Aydillo, A.J. Ruiz, M.Á. Toro, K.J. Gutiérrez, V.M. Merino, A. Cornejo, J.A. Palop, C. Sanmartín, D. Plano, Synthesis and Leishmanicidal activity of novel urea, thiourea, and selenourea derivatives of diselenides, Antimicrob, e02200-18(1-16), Agents Chemother. 63 (2019), https://doi.org/10.1128/AAC.02200-18.

[28] R. Tokala, S. Bale, I.P. Janrao, A. Vennela, N.P. Kumar, K.R. Senwar, C. Godugu, N. Shankaraiah, Synthesis of 1,2,4-triazole-linked urea/thiourea conjugates as

cytotoxic and apoptosis inducing agents, Bioorg. Med. Chem. Lett. 28 (2018) 1919–1924, https://doi.org/10.1016/j.bmcl.2018.03.074.
[29] H. Hu, C. Lin, M. Ao, Y. Ji, B. Tang, X. Zhou, M. Fang, J.Z. Zeng, Wu Synthesis and biological evaluation of 1-(2-(adamantane-1-yl)-1*H*-indol-5-yl)-3-substituted urea/thiourea derivatives as anticancer agents, RSC Adv. 7 (2017) 51640–51651 http://xlink.rsc.org/?DOI=c7ra08149a.
[30] F. Azam, Synthesis of some urea and thiourea derivatives of naphtha[1,2-*d*]thiazol-2-amine as anti-Parkinsonian agents that cause neuroprotection against haloperidol-induced oxidative stress in mice, Med. Chem. Res. 18 (2009) 287–308, https://doi.org/10.1007/s00044-008-9127-y.
[31] A. Rifati Nixha, A. Ergun, N. Gencer, O. Arslan, M. Arslan, Development of carbazole-bearing pyridopyrimidine-substituted urea/thiourea as polyphenol oxidase inhibitors: synthesis, biochemistry, and theoretical studies, Arch. Physiol. Biochem. 125 (2018) 263–269, https://doi.org/10.1080/13813455.2018.1453523.
[32] A. Sharma, R. Suhas, K.V. Chandana, S.H. Banu, D.C. Gowda, tert-Butyl 1,5-bis(4-(benzo[*d*]isothiazol-3-yl)piperazin-1-yl)-1,5-dioxopentan-2-ylcarbamate urea/thiourea derivatives as potent H+/K+-ATPase inhibitors, Bioorg. Med. Chem. Lett. 23 (2013) 4096–4098, https://doi.org/10.1016/j.bmcl.2013.05.043.
[33] M. Chayah, M.D. Carriûn, M.A. Gallo, R. Jimènez, J. Duarte, M.E. Camacho, Development of urea and thiourea Kynurenamine derivatives: Synthesis, molecular modeling, and biological evaluation as nitric oxide synthase inhibitors, ChemMedChem 10 (5) (2015) 874–882, https://doi.org/10.1002/cmdc.201500007.
[34] Kanwal, M. Khan, Arshia, K.M. Khan, S. Praveen, M. Shaikh, N. Fatima, M.I. Choudhary, Syntheses, *in vitro* urease inhibitory activities of urea and thiourea derivatives of tryptamine, their molecular docking and cytotoxic studies, Bioorg. Chem. 83 (2019) 595–610, https://doi.org/10.1016/j.bioorg.2018.10.070.
[35] M. Colamartino, L. Padua, C. Meneghini, S. Leone, T. Cornetta, A. Testa, R. Cozzi, Protective effects of L-Dopa and Carbidopa combined treatments on human catecholaminergic cells, DNA Cell Biol. 31 (2012) 1572–1579, https://doi.org/10.1089/dna.2011.1546.
[36] J. Solecka, A. Guśpiel, M. Postek, J. Ziemska, R. Kawęcki, K. Łęczycka, A. Osior, B. Pietrzak, K. Pypowski, A. Wyrzykowska, New derivatives of 3,4-dihydroisoquinoline-3-carboxylic acid with free-radical scavenging, *D*-amino acid oxidase, acetylcholinesterase and butyrylcholinesterase inhibitory activity, Molecules 19 (2014) 15866–15890, https://doi.org/10.3390/molecules191015866.
[37] W.S. Saari, Antihypertensive amino acid esters, US4038411A, 1977. http://patft.uspto.gov/netacgi/nph-Parser?Sect1=PTO1&Sect2=HITOFF&d=PALL&p=1&u=%2Fnetahtml%2FPTO%2Fsrchnum.htm&r=1&f=G&l=50&s1=4038411.PN.&OS=PN/4038411&RS=PN/4038411.
[38] W. Cawello, H. Boekens, J. Waitzinger, U. Miller, Moexipril shows a long duration of action related to an extended pharmacokinetic half-life and prolonged ACE inhibition, Int. J. Clin. Pharm. Ther. 40 (2002) 9–17, https://doi.org/10.5414/cpp40009.
[39] J. Tan, J.M. Wang, F.H.H. Leenen, Inhibition of brain angiotensin-converting enzyme by peripheral administration of trandolapril versus lisinopril in Wistar rats, Am. J. Hypertens. 18 (2005) 158–164, https://doi.org/10.1016/j.amjhyper.2004.09.004.
[40] Anderson, Prodrug Approaches for Drug Delivery to the Brain, in: B.D.V. Stella, R. Borchardt, M. Hageman, R. Oliyai, H. Maag, J. Tilley (Eds.), Prodrugs: Challenges and Rewards, Springer-Verlag, New York, 2007, pp. 573-651. https://doi.org/10.1007/978-0-387-49785-3_17.
[41] P.A.V. Zwieten, Centrally Acting Antihypertensive Drugs - Present and Future, Clin. Exp. Hypertens. 21 (1999) 859–873, https://doi.org/10.3109/10641969909061015.
[42] Parkinson Study Group, DATATOP: A Multicenter Controlled Clinical Trial in Early Parkinson's Disease, Arch. Neurol. 46 (1989) 1052–1060, https://doi.org/10.1001/archneur.1989.00520460028009.
[43] M.D. Day, M.J. Rand, A possible mechanism of action for *α*-methyldopa (Aldomet), Int. J. of Neuropharmacol. 3 (1964) 173–175, https://doi.org/10.1016/0028-3908(64)90005-X.
[44] H. Uchino, Y. Kanai, D.K. Kim, M.F. Wempe, A. Chairoungdua, E. Morimoto, M.W. Anders, H. Endou, Transport of Amino Acid-Related Compounds Mediated by *L*-Type Amino Acid Transporter 1 (LAT1): Insights Into the Mechanisms of Substrate Recognition, Mol. Pharmacol. 61 (2002) 729–737, https://doi.org/10.1124/mol.61.4.729.
[45] N. Zerangue, LAT1 Transporters expressed in blood brain barrier cells, US7462459B2, 2008. http://patft.uspto.gov/netacgi/nph-Parser?Sect1=PTO1&Sect2=HITOFF&d=PALL&p=1&u=%2Fnetahtml%2FPTO%2Fsrchnum.htm&r=1&f=G&l=50&s1=7462459.PN.&OS=PN/7462459&RS=PN/7462459.
[46] P. Gurunanjappa, M.B. Ningappa, A.K. Kariyappa, Synthesis of pyrazole fused pyran analogues: Antimicrobial, antioxidant and molecular docking studies, Chem. Data Collect. 5–6 (2016) 1–11, https://doi.org/10.1016/j.cdc.2016.09.002.
[47] C. Semidalas, E. Semidalas, M.T. Matsoukas, C. Nixarlidis, P. Zoumpoulakis, *In silico* studies reveal the mechanisms behind the antioxidant and anti-inflammatory activities of hydroxytyrosol, Med. Chem. Res. 25 (2016) 2498–2511, https://doi.org/10.1007/s00044-016-1689-5.
[48] M. Jabeen, S. Ahmad, K. Shahid, A. Sadiq, U. Rashid, Ursolic acid hydrazide based organometallic complexes: synthesis, characterization, antibacterial, antioxidant, and docking studies, 65(1-14), Front. Chem. 6 (2018), https://doi.org/10.3389/fchem.2018.00055.
[49] R. Feng, X. Zhou, P.M.Y. Or, J.Y. Ma, X.S. Tan, J. Fu, C. Ma, J.G. Shi, C.T. Che, Y. Wang, J.H.K. Yeung, Enzyme kinetic and molecular docking studies on the metabolic interactions of 1-hydroxy-2,3,5-trimethoxy-xanthone, isolated from *Halenia elliptica D. Don*, with model probe substrates of human cytochrome P450 enzymes, Phytomedicine 19 (2012) 1125–1133, https://doi.org/10.1016/j.phymed.2012.06.009.
[50] M.A.G. Vargas, M.C.R. Hernández, N.M. Fonseca, I.P. Martínez, Y.F. Sabater, F.M. Ramos, 2-Acetyl-4-aminoresorcinol derivatives: synthesis, antioxidant activity and molecular docking studies, Med. Chem. Res. 27 (2018) 1186–1197, https://doi.org/10.1007/s00044-018-2139-3.
[51] A.T.E. Ardjani, S.M. Mekelleche, Analysis of the antioxidant activity of 4-(5-chloro-2-hydroxyphenylamino)-4-oxobut-2-enoic acid derivatives using quantum-chemistry descriptors and molecular docking, 302(1-11), J. Mol. Model. 22 (2016), https://doi.org/10.1007/s00894-016-3160-4.
[52] H. Gao, J. Li, D. Sivakumar, T.S. Kim, S.K.S. Patel, V.C. Kalia, I.W. Kim, Y.W. Zhang, J.K. Lee, NADH oxidase from *Lactobacillus reuteri*: A versatile enzyme for oxidized cofactor regeneration, Int. J. Biol. Macromol. 123 (2019) 629–636, https://doi.org/10.1016/j.ijbiomac.2018.11.096.
[53] Y.F.U. Eze, U.C. Okoro, D.I. Ugwu, S.N. Okafor, New carboxamides bearing benzenesulphonamides: synthesis, molecular docking and pharmacological properties, 103265(1-10), Bioorg. Chem. 92 (2019), https://doi.org/10.1016/j.bioorg.2019.103265.
[54] H.K. Kumara, R. Suhas, D.M.S. Vardhan, M. Shobha, D.C. Gowda, A correlation study of biological activity and molecular docking of Asp and Glu linked bishydrazones of quinazolinones, RSC Adv. 8 (2018) 10644–10653 http://xlink.rsc.org/?DOI=c8ra00531a.
[55] I.V. Komarov, S. Afonin, A.S. Ulrich, ^{19}F-Labeled amino acids for NMR structure analysis of membrane-bound peptides, in: G. Haufe, F.R. Leroux (Eds.), Fluorine in Life Sciences: Pharmaceuticals, Medicinal Diagnostics, and Agrochemicals, Academic Press, United States, 2019, pp. 349–395, , https://doi.org/10.1016/B978-0-12-812733-9.00010-6.
[56] T. Oprea, H. Matter, Integrating virtual screening in lead discovery, Curr. Opin. Chem. Biol. 8 (2004) 349–358, https://doi.org/10.1016/j.cbpa.2004.06.008.
[57] E. Fan, S.A.V. Arman, S. Kincaid, A.D. Hamilton, Molecular recognition: hydrogen-bonding receptors that function in highly competitive solvents, J. Am. Chem. Soc. 115 (1993) 369–370, https://doi.org/10.1021/ja00054a066.
[58] X. Liang, H. Pei, L. Ma, Y. Ran, J. Chen, G. Wang, L. Chen, Synthesis and Biological Evaluation of Novel Urea- and Guanidine-Based Derivatives for the Treatment of Obesity-Related Hepatic Steatosis, Molecules 19 (2014) 6163–6183, https://doi.org/10.3390/molecules19056163.
[59] N. Öztaskın, P. Taslimi, A. Maraş, İ. Gülcin, S. Göksu, Novel antioxidant bromophenols with acetylcholinesterase, butyrylcholinesterase and carbonic anhydrase inhibitory actions, Bioorg. Chem. 74 (2017) 104–114, https://doi.org/10.1016/j.bioorg.2017.07.010.
[60] N. Öztaşkın, Y. Çetinkaya, P. Taslimi, S. Göksu, İ. Gülçin, Antioxidant and acetylcholinesterase inhibition properties of novel bromophenol derivatives, Bioorg. Chem. 60 (2015) 49–57, https://doi.org/10.1016/j.bioorg.2015.04.006.
[61] N. Öztaşkın, R. Kaya, A. Maraş, E. Şahin, İ. Gülcin, S. Göksu, Synthesis and characterization of novel bromophenols: Determination of their anticholinergic, antidiabetic and antioxidant activities, Bioorg. Chem. 87 (2019) 91–102, https://doi.org/10.1016/j.bioorg.2019.03.010.
[62] S.B. Kedare, R.P. Singh, Genesis and development of DPPH method of antioxidant assay, J. Food Sci. Technol. 48 (2011) 412–422, https://doi.org/10.1007/s13197-011-0251-1.
[63] M. Cuendet, K. Hostettmann, O. Potterat, W. Dyatmiko, Iridoid Glucosides with Free Radical Scavenging Properties from Fagraea blumei, Helvetica 80 (1997) 1144–1152, https://doi.org/10.1002/hlca.19970800411.
[64] L. Marcocci, L. Packer, M.T.D. Lefaix, A. Sekaki, M.G. Albert, Antioxidant action of Ginkgo biloba extract EGb 761, Methods Enzymol. 234 (1994) 462–475, https://doi.org/10.1016/0076-6879(94)34117-6.
[65] E.J. Park, S. Cheenpracha, Leng C. Chang, T.P. Kondratyuk, J.M. Pezzuto, Inhibition of lipopolysaccharide-induced cyclooxygenase-2 and inducible nitric oxide synthase expression by 4-[(2'-O-acetyl-*α*-*L*-rhamnosyloxy)benzyl]isothiocyanate from Moringa oleifera, Nutr. Cancer. 63 (2011) 971–982, https://doi.org/10.1080/01635581.2011.589960.
[66] M. Burits, F. Bucar, Antioxidant activity of *Nigella sativa* essential oil, Phytother. Res. 14 (2000) 323–328, https://doi.org/10.1002/1099-1573(200008)14:5%3C323::AID-PTR621%3E3.0.CO;2-Q.
[67] B. Hazra, S. Biswas, N. Mandal, Antioxidant and free radical scavenging activity of Spondias pinnata, 63(1-20), BMC Complem. Altern. M. 8 (2008).
[68] H. Sudhamani, S.K.T. Basha, N. Venkateswarlu, T. Vijaya, C. Nagaraju, Synthesis and characterization of new thiourea and urea derivatives of 6-fluoro-3-(piperidin-4-yl)benzo[*d*] isoxazole: *In vitro* Antimicrobial and Antioxidant activity, J. Chem. Sci. 10 (2015) 1739–1746 https://www.ias.ac.in/article/fulltext/jcsc/127/10/1739-1746.
[69] http://www.swissdock.ch/docking (accessed 20 November 2019).
[70] E.F. Pettersen, T.D. Goddard, C.C. Huang, G.S. Couch, D.M. Greenblatt, E.C. Meng, T.E. Ferrin, UCSF Chimeraea visualization system for exploratory research and analysis, J. Computat. Chem. 25 (2004) 1605–1612, https://doi.org/10.1002/jcc.20084.
[71] http://preadmet.bmdrc.org/ (accessed 20 December 2019).
[72] http://www.molinspiration.com/cgi-bin/properties (accessed 10 December 2019).
[73] http://www.organic-chemistry.org/prog/peo/ (accessed 01 December 2019).